

2005

Floor vibration control using three-degree-of-freedom tuned mass dampers

Khalid Ibraheem Al-Hulwah
University of Dayton

Follow this and additional works at: https://ecommons.udayton.edu/graduate_theses

Recommended Citation

Al-Hulwah, Khalid Ibraheem, "Floor vibration control using three-degree-of-freedom tuned mass dampers" (2005). *Graduate Theses and Dissertations*. 75.
https://ecommons.udayton.edu/graduate_theses/75

This Dissertation is brought to you for free and open access by the Theses and Dissertations at eCommons. It has been accepted for inclusion in Graduate Theses and Dissertations by an authorized administrator of eCommons. For more information, please contact mschlange1@udayton.edu, ecommons@udayton.edu.

FLOOR VIBRATION CONTROL USING
THREE-DEGREE-OF-FREEDOM
TUNED MASS DAMPERS

Dissertation

Submitted to

The School of Engineering of the
UNIVERSITY OF DAYTON

in Partial Fulfillment of the Requirements for
The Degree
Doctor of Philosophy in Mechanical Engineering

by

Khalid Ibraheem Al-Hulwah

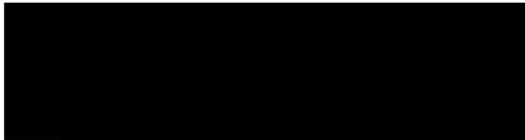
UNIVERSITY OF DAYTON

Dayton, Ohio

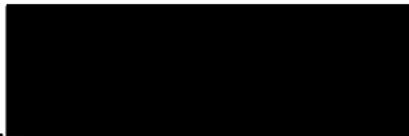
August 2005

FLOOR VIBRATION CONTROL USING THREE-DEGREE-OF-FREEDOM TUNED MASS DAMPERS

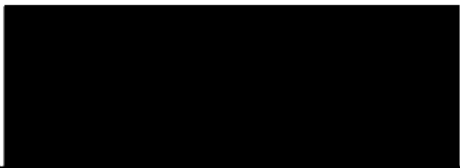
APPROVED BY:



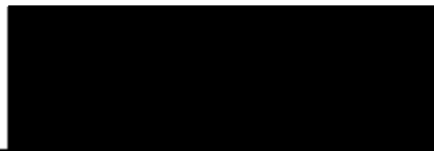
Reza Kashani, Ph.D.
Professor
Committee Chairperson
Department of Mechanical and
Aerospace Engineering



Manoochehr Zoghi, Ph.D.
Associate Professor
Committee Member
Department of Civil and
Environmental Engineering



Michael Turner, Ph.D.
Assistant Professor
Committee member
Department of Mechanical and
Aerospace Engineering



Taan ElAli, Ph.D.
Adjunct Faculty
Committee Member
Department of Electrical and
Computer Engineering



Donald L. Moon, Ph.D.
Associate Dean
Graduate Engineering Programs
and Research
School of Engineering



Joseph Saliba, Ph.D., P.E.
Dean
School of Engineering

© Copyright by
Khalid Ibraheem Al-Hulwah
All rights reserved
2005

ABSTRACT

FLOOR VIBRATION CONTROL USING THREE-DEGREE-OF-FREEDOM TUNED MASS DAMPERS

Khalid I. Al-Hulwah
The University of Dayton

Advisor: Dr. Reza Kashani

Floor vibration has become a serious structural problem for the occupants of some modern buildings. Transient floor vibration due to the normal activities (e.g., walking) of occupants in a typical office building with a steel frame has been investigated in this research. Such floor motion can be excessive and very annoying to occupants. To attenuate this excessive vibration, several remedial vibration-control methods are available (adding framing members, thickening the floor, etc.) but are not easy to implement in existing floors.

One of the most effective, passive vibration-treatment methods for reducing floor vibration is the use of the tuned mass damper. A new design of a tuned mass damper with three degrees of freedom and a unique configuration is proposed in this research; i.e., the three-degree-of-freedom tuned mass damper (3-DOF TMD). Due to its new configuration, the proposed TMD can fit easily into the ceiling cavities of most floor systems. Unlike the typical TMD, which commonly requires a large amount of viscous

damping, the 3-DOF TMD needs only a small amount of damping. Thus, the damping can be introduced into the proposed system through viscoelastic damping material.

The main purpose of this work has been to conduct analytical and experimental studies on the use of the 3-DOF TMD to abate floor vibration. In our studies to improve the dynamic behavior of the floor, a single 3-DOF TMD was tuned to the first vibration mode of the floor. For the floor system with this new TMD, the numerical simulation with both MATLAB and ANSYS showed an increase in the first-mode damping ratio from 0.5% to about 7.5%. To verify the effectiveness of the proposed TMD experimentally, a scale model of the floor was designed and constructed. After installing the 3-DOF TMD on the floor scale model, the equivalent damping ratio of the first mode increased from 5.8 to about 12%. The 3-DOF TMD proved analytically and experimentally to be very effective in providing additional damping to the target vibration mode and reducing the floor vibration.

ACKNOWLEDGMENTS

The completion of my dissertation would not have been possible without the help of many people, both professionally and personally.

On the professional side, I thank my advisor, Dr. Reza Kashani, for his tremendous support and encouragement during my Ph.D. degree. I also thank the rest of my Ph.D. committee members--Dr. Manoochehr Zoghi, Dr. Michael Turner, and Dr. Taan ElAli--for participating on the committee and helping me in the research. My extra-special appreciation goes to both Dr. Joseph Saliba, who was on my committee earlier and shared many suggestions, and Dr. Robert Brockman, who taught me the finite-element analysis courses (FEA I and II) and has provided much assistance with ANSYS. In addition, I am grateful to Larry Collins, who helped in some of the experimental work.

On a personal basis, heartfelt appreciation goes to my wife, Maha, for her patience, help and encouragement, and to my two children, Shoug and Faris, for their patience. I also thank all of my brothers and sisters, especially my brothers Dr. Mohammed and Hammood, because they have always encouraged me in my study. Furthermore, in deep appreciation of my mother's sacrifices, I dedicate this work to her.

To the rest of the people who have helped and supported me, I am deeply grateful.

TABLE OF CONTENTS

	Page
ABSTRACT.....	iii
ACKNOWLEDGMENTS	v
LIST OF ILLUSTRATIONS	viii
LIST OF TABLES	x
 CHAPTER	
I. INTRODUCTION AND LITERATURE REVIEW	1
1.1 Literature Review	2
1.1.1 Floor Vibration: Background	2
1.1.2 Passive and Active Methods for Reducing Floor Vibrations	8
1.1.3 Tuned Mass Damper and Its Application	8
1.1.4 The Use of Tuned Mass Damper to Control Floor Vibration	9
1.2 Research Overview	13
II. TYPICAL OFFICE FLOORS	15
2.1 Floor Modal Parameters	17
2.1.1 Experimental Results	17
2.1.2 Finite-Element Model	18
2.2 Analytical Model of the Floor	21
2.2.1 Multi-Degree-of-Freedom Floor Model	21
2.2.2 Single-Degree-of-Freedom Floor Model	23
2.3 Floor Excitation and Type of Response	23
2.4 Evaluating Floor Vibrations	24
III. THE USE OF A THREE-DEGREE-OF-FREEDOM TUNED MASS DAMPER TO CONTROL FLOOR VIBRATIONS	27
3.1 Optimal Design of Tuned Mass Damper	28
3.2 The Proposed Three-Degree-of-Freedom Tuned Mass Damper	32

3.3 Design of a 3-DOF TMD to Control Floor Vibration	34
3.3.1 The Configuration of the 3-DOF TMD	42
3.3.2 The Finite-Element Analysis	46
3.4 Introduction of Damping to the Absorbers	53
IV. BUILDING A SCALE MODEL OF THE FLOOR	56
4.1 The Wooden Scale Model of the VPI Floor	57
4.1.1 An Initial Scale Model of the Floor	57
4.1.1.1 Beam Scaling	58
4.1.1.2 Plate Scaling	61
4.1.1.3 Column Scaling	66
4.1.2 Rescaling the Initial Scale Model of the Floor	66
4.1.3 The Final Scale Model of the Floor	68
4.1.3.1 The Actual Floor Frequencies	71
4.2 The Steel Scale Model of the VPI Floor	77
V. EXPERIMENTAL RESULTS	81
5.1 Absorbers	83
5.2 The 3-DOF TMD	87
5.2.1 Absorber Components	97
5.3 Tuning of the 3-DOF TMD	100
VI. SUMMARY, CONCLUSIONS, AND RECOMMENDATIONS .	103
6.1 Summary	103
6.2 Conclusions	105
6.3 Recommendations	106
REFERENCES	107

LIST OF ILLUSTRATIONS

Figure 1.1	Reiher-Meister and Modified Reiher-Meister Scales	6
Figure 2.1	Top View of the Floor Plan	16
Figure 2.2	Natural Frequencies and Mode Shapes of the Finite-Element Model ...	20
Figure 2.3	Heel-Drop Impact	24
Figure 2.4	Modified Reiher-Meister Scale.....	26
Figure 3.1	A SDOF TMD Attached to a SDOF Floor Model.....	28
Figure 3.2	Magnitude of the FRFs mapping force to the displacement at the center of the floor.....	35
Figure 3.3	Simulation block diagram.....	37
Figure 3.4	Magnitude of the FRFs' mapping force to the displacement at the center of the floor.....	39
Figure 3.5	Transient response at the center of the floor to a heel-drop Impact.....	41
Figure 3.6	The 3-DOF TMD	43
Figure 3.7	Equivalent Spring and Mass	45
Figure 3.8	The Finite-Element Mesh of the Floor With the 3-DOF TMD	50
Figure 3.9	The Frequency Response of the Floor With and Without the 3-DOF TMD (No Damping)	51

Figure 3.10	The Frequency Response of the Combined System With and Without 1% Damping in Each Absorber.....	52
Figure 3.11	A Constrained-Layer Damping.....	55
Figure 4.1	Top View of the Wooden Frame of the Final Floor Scale Model	71
Figure 4.2	The First Five Mode Shapes of the Floor Finite-Element Scale Model	74
Figure 4.3	The Wooden Scale Model of the VPI Floor with the Added Masses....	75
Figure 4.4	The Experimental Frequency Response of the Floor Scale Model.....	76
Figure 4.5	The Steel Scale Model of the VPI Floor.....	78
Figure 5.1	Absorber Without and With Coulomb Damping.....	84
Figure 5.2	Absorber Without and With Viscoelastic Material.....	86
Figure 5.3	Frequency Response of the Floor Scale Model	88
Figure 5.4	Frequency Response Magnitude of the Floor Model With and Without the 3-DOF TMD	92
Figure 5.5	Full and Effective Lengths for the Cantilevered Beam	95
Figure 5.6	The Absorber's Components	97
Figure 5.7	The 3-DOF TMD on the Floor Model	99
Figure 5.8	Frequency Response Magnitude of the Floor Model With and Without the 3-DOF TMD	102
Figure 5.9	Frequency Response Magnitude of the Floor Model With and Without the 3-DOF TMD	102

LIST OF TABLES

Table 2.1	Experimental Floor Data by Hanagan (1994).....	18
Table 3.1	Simulation Parameters	40
Table 3.2	Initial Design Parameters of the 3-DOF TMD	48
Table 4.1	The Given and the Computed Material Information.....	65
Table 4.2	Initial Scaling Factors	65
Table 4.3	Rescaling Factors	68
Table 4.4	Final Scaling Factors.....	69
Table 4.5	Geometric Properties of the Real Beams	70
Table 4.6	Geometric Properties of the Scaled Beams.....	70
Table 4.7	Final Scaling Factors.....	78
Table 4.8	The Final Dimensions of the Scaled Beams	78
Table 5.1	Experimental Floor Modal Parameters	89
Table 5.2	3-DOF TMD Absorbers' Parameters.....	92
Table 5.3	Initial Design Parameters of the 3-DOF TMD	94

CHAPTER I

INTRODUCTION AND LITERATURE REVIEW

One of the important problems facing occupants, designers, and owners of modern buildings is excessive floor vibration. Because modern floors with steel frames and concrete slabs contain high-strength materials and extend across a wider span, they tend to be more flexible and more oscillatory. Lightweight floors with large open areas and without partitions vibrate with very low damping. With these being floors common in office buildings, shopping centers, and schools, this vibration understandably is a source of annoyance for many people. The vibration can be induced by many sources; human activity (e.g., walking, running) and operating machines are the two most common.

Several researchers have studied floors that exhibit annoying motion and proposed a number of methods for reducing floor vibration. Such methods are based on either stiffening or adding dissipative damping to the floor. The stiffening approach and some damping techniques, such as installing full-height partitions, adding framing members, thickening the floor, or adding damping posts, are both costly to install in a new building and very difficult to implement in an existing building. Reactive damping,

provided by attaching tuned mass dampers (TMDs) to floors, is more readily implementable.

The purpose of this work is to develop a new design of a three-degree-of-freedom tuned mass damper (3-DOF TMD) to attenuate excessive vibration of an office-type floor with steel frame due to normal occupant activity, e.g., walking.

1.1 Literature Review

1.1.1 Floor Vibration: Background

A floor is a sophisticated, dynamic system. As a continuous system, it has an infinite number of degrees of freedom with an infinite number of modes of vibration. For each mode of vibration, there is a corresponding natural frequency, mode shape, and damping ratio. However, like most of the real physical systems, only a limited number of modes of vibration within a specific frequency range are of great concern. The first few modes, which are normally in the frequency range under 20 Hertz (Hz), are dominant and contribute more energy to the bending vibration of the floor. The first and most important mode, called the fundamental mode, has the lowest natural frequency and the largest displacement.

Human activity excites floors at the first few natural frequencies. Their movements on the floor usually have forcing frequencies in the range of 1.5 to 3.2 Hz [1]. For instance, their walking movement has a forcing frequency of about 2 Hz. This movement excites a vibratory motion in the flexible floor. When a harmonic of human excitation is very close to one of the natural frequencies of the floor, especially the fundamental one, extreme floor oscillation results from the resonance condition. Many

cases in the literature have discussed severe floor vibrations due to this resonance. For example, both Setareh [2] and Webster and Vaicaitis [3] reported excessive floor vibration because the forcing frequency matched the fundamental frequency of the floor at about 2.4 Hz.

Humans are known to be very sensitive to some degree of floor vibration [8]. Sensitivity of an occupant to vibration relies on the distance between the occupant and the source of vibration, activity around the occupant, and the movement and position of the occupant [5, 8]. Floor vibration with a small amplitude of only four hundredths of an inch may become aggravating to occupants [4]. The floor vibration affects not only the comfort of the occupants but also any sensitive equipment that might be on the floor. Excessive floor vibration can cause some equipment to malfunction.

Floors that vibrate at a particular frequency range subject the occupants to an annoying motion. Floors that are most disturbing to people often have low resonant frequencies. Murray [4] studied more than 100 existing residential and office floors and found that the floor fundamental frequency usually is in the range of 5 to 8 Hz. Additionally, Murray [4] analyzed more than 50 residential and office floors with annoying motion and found that the fundamental frequency for most of them also is in the range of 5 to 8 Hz. Coincidentally, the natural frequencies of internal human organs also fall between 5 and 8 Hz [5]. With that in mind, if a floor frequency and a harmonic of the forcing function fall close together within the frequency range of 5 to 8 Hz, the resonance occurs for both the floor system and the internal organs of the occupants. This resonance results in floor motion that is excessive and very irritating to the occupants [6, 7].

Because of the importance of the floor oscillation and the consequences of neglecting the dynamic behavior of the floor, the floor-vibration problem has gained more attention and still concerns many researchers. A great deal of work has been done in this area, especially in analyzing floor vibration. The outcomes of some of the more important works are summarized here.

Typically, floor response can be classified as either transient or steady-state, depending upon the type of excitation and its duration. Floors subject to operating machines have a steady-state response because machines usually run continuously for a long period of time. Excessive floor motion due to machinery can be reduced by isolating the offending machine. Conversely, floor response to occupant activity cannot easily be categorized as being transient or steady-state unless the floor environment is well defined. Many researchers have studied floor vibrations of several types of floor environments and proposed guidelines (building floor vibrations), scales (Modified Reiher-Meister scale), and criteria (Murray criteria) for evaluating floors' structural motion.

Murray [4] described three types of floor environments: residence/office, commercial building (shopping center), and gymnasium. For the residential and office type of environment, Murray [4] noted that the excitation is the intermittent movement of a small number of occupants; therefore, the floor oscillation is transient. Consequently, the amount of damping in the floor has a strong influence on the floor vibration in this type of environment. The typical test excitation for examining the vibration of the residential and office floors is the heel-drop impact. The heel-drop impact is the dynamic

load of a 190-lb. person who stands on the toes of both feet, then strikes the floor with both heels from a distance of 2 in. [5, 9].

Regarding the commercial environment, Murray [4] reported that the floor response is steady-state because the excitation is approximately the constant movement of walking or running. For the final environment of the gymnasium, he noticed that the forcing function is that of dancing or exercise activities; hence, the floor vibration is steady-state. The sinusoidal function is the normal test input for analyzing both commercial and gymnasium environments.

Human perception of vibration has been investigated by several researchers, such as Reiher and Meister [30], and Lenzen [10]. In 1931 Reiher and Meister [30] studied human reaction to steady-state vibration and produced the Reiher-Meister scale. This well-known scale is shown in Figure 1 (A). Three decades later, Lenzen [10] conducted experiments to study human response to floor transient vibration and developed the modified Reiher-Meister scale. This scale is shown in Figure 1 (B). From these two trusted scales, it is clear that humans are more sensitive to steady-state vibration than to transient vibration. In both scales, the evaluation of human perception to the vibrations depends on the floor's displacement amplitude (in.) and frequency (Hz).

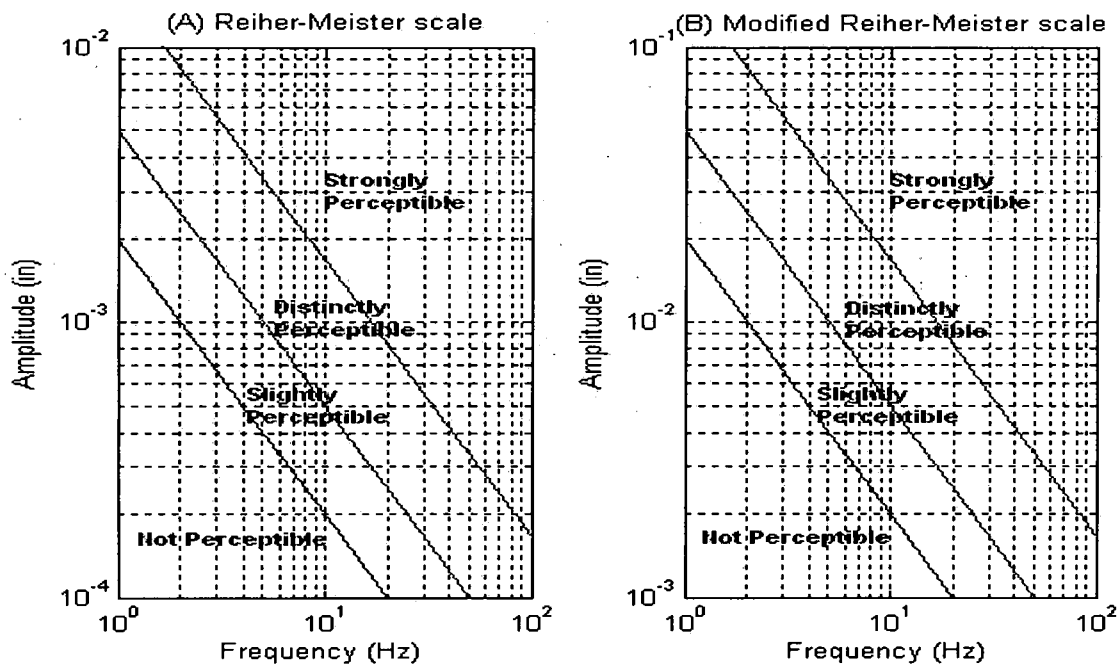


Figure 1.1: Reiher-Meister and Modified Reiher-Meister Scales

Among the three transient vibration factors (i.e., frequency, amplitude, and damping), which were considered in the experimental evaluation of human reaction to the floor transient response, Lenzen [10] reached the conclusion that the amount of damping presented in the floor system was the most important. Most of the real floor systems have damping to some degree. As a result, the amplitude of vibration gradually decreases and the energy is dissipated in the form of heat [11]. The damping indicates the time required for the oscillation to die out or, more quantitatively, the number of cycles needed before the vibration will end.

Lenzen [10] also found that the occupants would sense only the initial impact if the floor response diminishes within the first four cycles of oscillation. In the case that the amplitude of vibration after five cycles is less than twenty percent of the initial amplitude, the floor vibration is barely perceptible, or not perceptible at all. He reported

that the floor vibration is between perceptible and barely perceptible if the amplitude after five cycles is within the range of 20 and 40 percent of the initial amplitude. In the case that the amplitude after five cycles of vibration was more than 40 percent of the initial amplitude, floor oscillations were definitely perceptible. Lenzen [10] concluded that the occupant reacted to the vibration as a steady-state vibration if the floor oscillation continued for more than 12 cycles.

One of the most important criteria to evaluate the vibration of a steel floor is the Murray criterion. Murray [4] developed his criterion to assess the floor vibration of an office or a residential environment due to the walking of occupants. This assessment can help the structural-design engineer to check the serviceability limit states of the proposed floor design. In other words, it predicts the levels of vibration in the floor with respect to the occupants. Also, this criterion can assist the vibration-control engineer to evaluate the level of floor vibration after the construction. For an acceptable floor system with a fundamental frequency less than 10 Hz, the following inequality should be met [4, 12]:

$$D > 35 A_0 f + 2.5$$

where D = Estimated damping of the floor (%)

A_0 = Maximum amplitude of the floor vibration due to a heel-drop impact (in.)

f = First resonant frequency of the floor (Hz).

Estimated damping, maximum amplitude, and floor fundamental frequency are necessary parameters that need to be determined. Because the computations of the maximum amplitude and the floor first frequency are lengthy and need to be accurate, some commercially available software (e.g., FLOORVIB, Software) can help to compute these parameters. Murray [4] and Hanagan and Murray [12] discussed this and other criteria in

details, giving many examples and providing more information about the estimated damping.

Several researchers have studied floor systems that have annoying motion and, as a result, have produced the following passive and active vibration-treatment methods.

1.1.2 Passive and Active Methods for Reducing Floor Vibrations

Unwanted floor vibration due to occupant normal activity can be reduced by several active and passive vibration-control methods. Active control methods need external energy sources, whereas passive methods do not need such sources and depend only upon the device's reaction [6]. Hanagan [5] reported successful installations of active vibration control with a proof-mass actuator in seven different floors. Many traditional (passive) methods are available for reducing floor vibration. They include installing full-height partitions, adding damping posts, stiffening the structure of framing members, adding to the concrete thickness, and attaching tuned mass dampers to the floor [5].

1.1.3 Tuned Mass Damper and Its Applications

A tuned mass damper (TMD), or vibration absorber (VA), which was invented in 1911 by Frahm, is a spring-mass-dashpot system. It has been used in several applications to reduce vibration, such as for machines that operate with constant frequency, tall buildings that sway, and power-transmission lines with flow-induced vibration. Huge TMDs usually are used to suppress wind-induced vibration in very tall buildings. For instance, a TMD that weighs 400 tons is employed to control the first mode of the sway motion of the Citicorp Center in New York [13]. Literature is filled with similar applications.

With the new development in the configuration of TMD and the optimization of parameters, the addition of a TMD to the floor is an effective method to increase damping. The goal of using this mechanical device, as suggested by Lenzen [10], is to reduce the floor's transient response to a small amplitude within the first four cycles of floor vibration so that occupants experience only the foot impact, not the floor response.

1.1.4 The Use of Tuned Mass Damper to Control Floor Vibration

One of the most effective, passive vibration-control techniques to abate annoying floor vibration is to add a TMD to the floor system. In the past several decades, numerous researchers have successfully reduced floor transient vibration by using TMD. For example, Lenzen [10] used a TMD to control a single mode of vibration. Shope and Murray [14], as well as Rottmann [6], used several TMDs to control a few modes of vibration.

Lenzen [10] used a TMD to reduce the vibration of a laboratory test floor. A simple spring-mass-dashpot system with a frequency of 1 Hz less than the floor's first resonant frequency was added to the floor to increase damping. A TMD with 0.02 of the floor mass and a damping ratio of 7.5 percent was able to reduce the vibration of the floor. Therefore, the response of the floor was diminished in less than five cycles.

Shope and Murray [14] employed TMDs to abate the vibration of an office floor that had four bays. In fact, they introduced a new design of TMD. This TMD consists of a multi-celled liquid damping device, steel weights, and a steel plate. The damping device and the steel weights are supported by the steel plate, which behaves as a spring. The measured natural frequencies at the center of a bay of the steel floor were 5.13 and 6.5 Hz

[6]. Also, the measured frequency at an edge of a bay was 5.25 Hz [6]. Fourteen TMDs were used to control two modes in three bays of the second floor. As a result, significant improvement in the floor vibration was obtained.

Another case study of installing TMDs with a new configuration was discussed by Rottmann [6]. She utilized TMDs to attenuate the vibration of an experimental test floor. The first three resonant frequencies of the floor were 7.375, 9.375, and 16.75 Hz. Three prototype TMDs, which had masses ranging from 5.8% to 11.93% of the floor modal masses (corresponding to the targeted modes), were used to control the first three modes of vibration. 3M Company designed the three TMDs, each of which consisted of four springs, a damping element, steel plates, and inner and outer frames. With these TMDs, the floor vibration was satisfactory.

Others, such as Setareh and Hanson [2], Webster and Vaicaitis [3], and Velivasakis [1], have tried to suppress steady-state floor vibration. Those researchers reported excessive and annoying floor vibrations because in each case study a harmonic of the forcing function coincided with the fundamental frequency of the floor.

Setareh and Hanson [2] used TMDs to suppress the floor vibration of an auditorium balcony. The floor had the first two modes at the frequencies 2.55 and 3.68 Hz; the damping ratio of the first mode was about 1.6%. Because human movements excited the fundamental frequency of this floor, resonance occurred with large vibration amplitudes. Each TMD consisted of a typical spring, mass and dashpot. Three 4000-lb. TMDs were designed to control the first mode, and two 2000-lb. TMDs were designed to control the second mode. With the TMDs, the amplitudes of the steady-state vibration

decreased to about 22%, and the first mode damping ratio of the floor increased from 1.6% to 8%.

Webster and Vaicaitis [3] employed TMDs to control the vibration of a long-span, cantilevered, composite floor. This floor was used for dining and dancing. The floor's first resonant frequency was about 2.3 Hz, and its damping ratio was about 3.2%. Because the dancing excited the first mode, four TMDs were placed at four appropriate positions of the floor to control the first mode. As a result, the TMDs decreased the vibration by at least 60%. The cost of the four TMDs was \$220,000.

Velivasakis [1] utilized TMDs to reduce the floor vibration of a school gymnasium. The school was constructed mostly of reinforced concrete. The gymnasium on the third floor had the first four resonant frequencies of 4, 4.6, 5.3, and 6.2 Hz, and the damping ratios ranged from 1.7% to 0.9%. When the school used the gymnasium, excessive floor vibration was noticed in both the second and the third floors. Therefore, eight TMDs were used to control the first four modes of vibration of the gym floor. Afterward, the accelerations for both the second and the third floors were decreased by greater than a factor of two. The total cost of the TMDs was \$500,000.

Hanagan and Murray [12] used an active vibration control with a proof-mass actuator (known also as active TMD) to provide reactive damping to the floor system. This control system in the form of velocity (rate) feedback used the output of the velocity sensor to develop the actuator force. The actuator was placed at the center of the floor to attenuate the maximum amplitude (antinode) of the first mode. This active vibration scheme was quite effective in reducing the transient vibration in an experimental test floor (an office-type floor). The damping ratio of the first mode increased from 2.2% to

40%. For walking excitation, the velocity amplitudes with active control decreased to about 12%. This control system also was used successfully by Hanagan [5] in six additional floors. The control system cost \$16,000 and requires more maintenance.

Both passive vibration control with TMD and active vibration control with proof-mass actuator provide artificial damping to the floor system. By comparison to other methods, passive vibration control via the addition of TMD has several advantages. First, its small size allows easy installation in a ceiling cavity or closet. Also, it can be installed permanently and requires less maintenance than active control. Finally, its cost is more reasonable than active control.

Another natural and unexpected system that has properties similar to the TMD is the human body. Both Lenzen [10] and Rottmann [6] did some experiments and reported that a group of occupants (e.g., 4 people, a class) has a great ability to absorb a significant amount of floor energy. Rottmann [6] found when four people were placed at the appropriate locations of a test floor, the damping ratio of the first mode increased by more than a factor of three. Also, Lenzen [10] reported that teachers complained about annoying vibration in a specific school after classes. Therefore, he performed some experimental tests in a classroom and observed that the amplitude after five cycles was 41.7% of the initial value with an empty classroom. Conversely, when the classroom was full, the amplitude after five cycles reduced to 8.7% of the initial value. Lenzen [10] found that concentrated rigid masses, such as concrete cylinders, do not provide more damping to the floor but instead decrease the floor damping. Thus, occupants are perfect dampers [15, 6, 10].

1.2 Research Overview

A sizeable amount of damping (typically a ratio of about 13%) is needed in a tuned mass damper in order to effectively add damping to a resonant mode of a structure. Considering that the tuned dampers used in floor-vibration abatement are rather massive, adding enough damping to them while keeping them small and affordable is a challenge. As an alternative, the use of a 3-DOF TMD is proposed.

The goal of this research is to conduct analytical and experimental studies on the use of three-degree-of-freedom tuned mass dampers (3-DOF TMDs) to abate floor vibration. Such TMDs can provide the same effectiveness as a traditional 1-DOF TMD without needing as much damping as a traditional TMD. As in a 1-DOF TMD, this device will be installed on a concrete floor slab, at an optimally designed/chosen location. The design of an effective vibration-control system via a 3-DOF TMD to abate floor vibration caused by occupant walking is discussed in this research.

The outline of the research is as follows. In Chapter 2, a full-scale floor that represents an office-type floor is described in detail. For the sake of comparison of our results with the ones existing in the literature, the experimental test floor at the Virginia Polytechnic Institute and State University (VPI) is used in the model. Both the modal testing results, which were obtained by Hanagan [5], and the finite-element results of the VPI floor are presented. Using this useful modal information, the analytical model of the floor system is constructed in that chapter. Chapter 3 starts with some basic concepts of the 1-DOF TMD. Then, the proposed 3-DOF TMD is introduced. The rest of that chapter covers the application of the 3-DOF TMD to the full-scale VPI floor model. Chapter 4 discusses the design and fabrication of a scale model of the VPI floor. Chapter 5 focuses

on the experimental work involved in developing a prototype of the 3-DOF TMD and on verifying the effectiveness of this mechanical device in reducing the vibration of the scale model of the floor. The summary and the conclusion are presented in Chapter 6.

CHAPTER II

TYPICAL OFFICE FLOORS

A type of floor construction that is frequently reported to have annoying vibration is a thin, lightweight concrete slab supported by open-web steel joists [5, 12, 8]. Even though this economical type of floor system can be used for many low-rise steel buildings, such as office buildings, schools, and restaurants, the objective of this research is to analyze the vibration of the steel joist-concrete slab floor system specifically in office buildings.

One such full-scale test floor that has been constructed, modeled, and studied analytically and experimentally at Virginia Polytechnic Institute and State University (VPI) is considered in this study. This floor is referred to as the VPI floor in the remaining part of this study. During the last ten years, more than twelve papers (e.g., Hanagan [5]; Rottmann [6]; Shope and Murray [14]; and Hanagan and Murray [12]) referred to the VPI floor as a typical office floor with annoying vibration. Hanagan [5] and Rottmann [6] described this floor system in detail in their theses.

This one-bay floor, which has a dimension of 25 ft. by 15 ft., is composed of a steel frame of two side girders (W14X22) and seven parallel joists (16K4) supporting a concrete slab on a metal deck. The lightweight concrete slab is 3.5 in. thick and is

supported by 1.0C metal deck [5]. The whole floor is supported at the corners by four steel pipe columns, each with a diameter of 8 in. Figure 2.1 shows the plan of this floor.

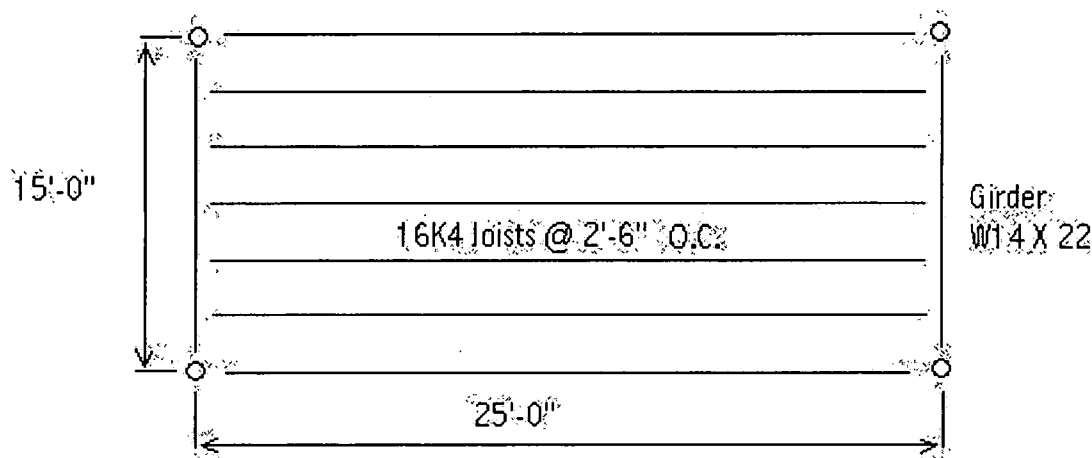


Figure 2.1: Top View of the Floor Plan [5]

The floor rests in the xy horizontal plane and vibrates up and down in the z direction. The transverse vibration $w(t,x,y)$ of the floor at any point is a function of both time (t) and position (x,y). The forcing function $f(t,x,y)$ at any point, like the transverse vibration, is a function of both time and position. For example, the dynamic-force input (human impact) and the floor dynamic response at the center of the VPI floor are $f(t, 12.5', 7.5')$ and $w(t, 12.5', 7.5')$, respectively.

As we previously noted in chapter one, the floor system, as a distributed-parameter system, possesses an infinite number of natural frequencies. To investigate the dynamic behavior of the floor system and to develop a theoretical model of it, only a finite number of natural frequencies need to be considered. For the VPI floor, Hanagan [5] suggested considering only the modes of vibration that have natural frequencies below 30 Hz. The reason for this suggestion is that the first four harmonics of walking

excitation can easily excite the floor's first few resonant modes, which occur below 30 Hz and dominate the floor response.

2.1 Floor Modal Parameters

In order to understand the dynamic behavior of the floor and to create a mathematical model of the floor, vibration characteristics of the floor should be determined. The necessary vibration characteristics, which are associated with the modes of vibration, are called the modal parameters. Experimental and analytical means need to be used in order to accurately determine the modal parameters of the VPI floor. Both the experimental modal analysis (EMA), also called modal testing, and the finite-element analysis (FEA) are very useful for analyzing the vibration of a complex structure and determining all modal parameters (natural frequencies, mode shapes, and damping ratios). The experimentally evaluated modal parameters are used to verify the results of the FEA.

2.1.1 Experimental Results

Hanagan [5] performed experimental vibration tests on the VPI floor, measured the frequency response, and extracted the modal data. As a result, she noticed that there were only five modes of vibration in the frequency range from 0 to 30 Hz. Also, she reported the measured natural frequencies and approximate modal damping ratios for these first five modes (see Table 2.1). Therefore, only the first five modes of vibration are considered in this analytical study. The damping ratios corresponding to the resonant frequencies were determined by the half-power method, which will be discussed in detail in chapter 5. This partial modal testing excluded the determination of the mode shapes

due to the difficulty of the task and the lack of sufficient test equipment (e.g., sensors, multichannel analyzer) for this enormous structure. Therefore, the mode shapes associated with these natural frequencies are obtained in the following section by FEA.

Table 2.1: Experimental Floor Data by Hanagan [5]

Mode	Frequency (Hz)	Damping Ratio (%)
1	7.3	0.5
2	9.4	0.85
3	16.5	0.85
4	16.9	0.5
5	26.5	0.55

2.1.2 Finite-Element Model

A floor system with a steel frame and concrete slabs (such as the VPI floor) has a complicated geometry. The dynamics of such a floor does not have a closed-form solution. As such, finite-element methods (FEMs) are used to model the floor and then to provide the modal parameters (e.g., mode shapes). The VPI floor is modeled in the ANSYS[®] finite-element analysis environment. Shell elements are used to model the composite of the metal deck and concrete slab, and beam elements are used to model the girders and joists.

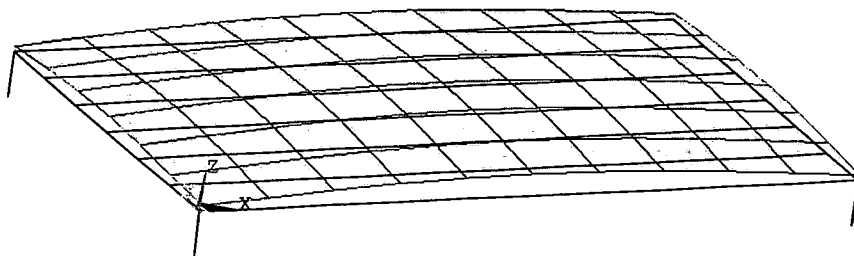
Hanagan and Murray [12] made great efforts to analyze the dynamic behavior of several steel floors, especially the VPI floor. They performed extensive analytical and experimental studies on the VPI floor. Hanagan and Murray [12] suggested a straightforward approach for modeling the floor system in the finite-element package by constructing the shell and beam elements in a single plane. Hanagan [5] described this as a grid model. Hanagan [5] did a series of static tests and numerous computations to

determine the precise structural properties of the VPI test floor. These material and geometric properties are used in the finite-element model of the VPI floor. As suggested by Hanagan and Murray [12], a mesh size of 30 in. by 30 in. is chosen for modeling the floor system. Hanagan [5] also noticed vertical motion at the four supports and suggested that the four columns be modeled as springs. Hanagan and Murray's practical suggestions are considered in the finite-element model of the VPI floor.

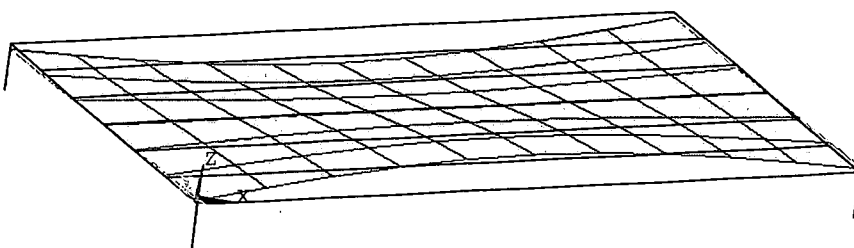
The finite-element model of the VPI floor is helpful for a comprehensive dynamic analysis (e.g., modal analysis, transient response, and harmonic response). To obtain the modal properties, the modal option is selected in ANSYS to solve the eigenvalue problem; as a consequence, the outcomes are both the eigenvalues (natural frequencies) and the eigenvectors (mode shapes). This precise finite-element floor model provides accurate natural frequencies and mode shapes. It gives almost a complete description of how the vibrating floor system is deformed at each natural frequency. Figure 2.2 shows the natural frequencies and mode shapes of the first five modes of the VPI floor finite-element model. The finite-element natural frequencies are similar to the experimental frequencies. The first mode shape at 7.16 Hz has the expected half-sine shape in the sides of the floor.

The pattern of the deformed shape at each natural frequency via ANSYS identifies the antinode, which is a point of maximum vibration amplitude [16]. Also, the mode shapes are helpful to determine the modal masses¹ of the floor system that correspond to each mode. As such, finite-element modeling is an important resource for studying the dynamic behavior of the floor system.

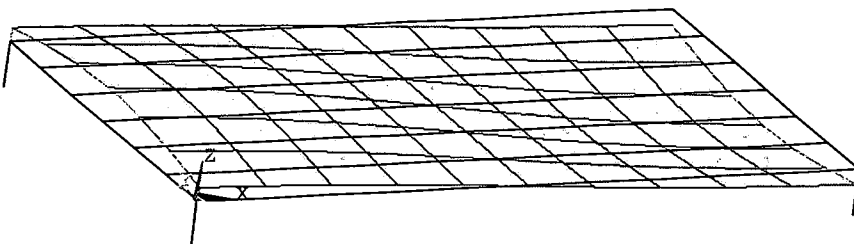
¹ N th modal mass of a structure is the mass used in modeling the N th mode of the structure as a 1 degree of freedom system.



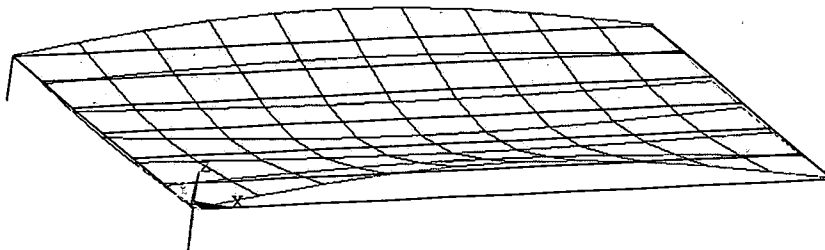
First Mode Shape at $f_1=7.16$ Hz



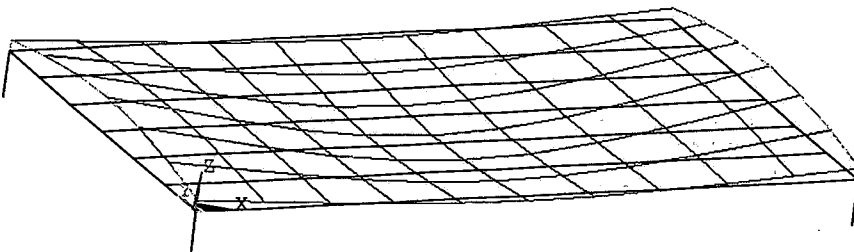
Second Mode Shape at $f_2=10.44$ Hz



Third Mode Shape at $f_3=15.90$ Hz



Fourth Mode Shape at $f_4=16.82$ Hz



Fifth Mode Shape at $f_5=26.40$ Hz

Figure 2.2: Natural Frequencies and Mode Shapes of the Finite-Element Model

2.2 Analytical Model of the Floor

2.2.1 Multi-Degree-of-Freedom Floor Model

In order to precisely describe the dynamic behavior of the VPI floor, a mathematical model must be constructed [17]. The VPI floor is a huge, complex structure consisting of many flexible structural components. The dynamic response of this distributed-parameter system depends upon the dynamic behavior of the individual structural components, such as the girders, joists, and concrete slab. Therefore, this floor-system response does not have a closed-form solution. Consequently, a lumped-parameter model that can predict the floor-system response is required. The modal parameters, which were determined previously by the vibration modal tests (natural frequencies and damping ratios) and the finite-element method (mode shapes), provide sufficient parameters for this Multi-DOF model. The lumped-parameter model that depends primarily on the modal parameters of the first five modes is usually called "modal model" and sometimes "five-mode model."

Modal-superposition method is used to obtain the forced response of the floor system. In this analytical approach, every normal (natural) mode of vibration is represented by a single, independent (decoupled) differential equation. The use of the first five vibration modes in this dynamic analysis results in five modal equations. This set of second-order linear modal differential equations is written in terms of principal (generalized) coordinates and can be solved easily. The floor-system response is obtained by superposition of the responses of the individual normal modes.

For convenience and computer use, these differential equations usually are expressed in matrix form. The matrix modal differential equation for a single input and a single output is

$$\ddot{\eta}(t) + 2 \zeta \Omega \dot{\eta}(t) + \Omega^2 \eta(t) = Q f(t) \quad (2.1)$$

where

the generalized coordinates, $\eta(t) = \{\eta_1, \eta_2, \eta_3, \eta_4, \eta_5\}$

the damping ratios, $\zeta = \text{diag}\{\zeta_1, \zeta_2, \zeta_3, \zeta_4, \zeta_5\}$

the natural frequencies, $\Omega = \text{diag}\{\omega_1, \omega_2, \omega_3, \omega_4, \omega_5\}$

the mode shapes, $Q = \{Q_1, Q_2, Q_3, Q_4, Q_5\}$, and

the floor-system response at the same point of the dynamic force input $f(t)$ is given by $w(t) = Q \eta(t)$; see Kashani [18].

The state-space form of the modal differential equation (Equation 2.1) should be developed to conveniently study the time-domain and the frequency-domain characteristics of the VPI floor system. The state-space representation in the software package MATLAB provides accurate numerical simulation. Using the natural frequencies, damping ratios, and mode shapes for the first five modes, the state-space model of the floor is constructed. Equations 2.2a and 2.2b show this model for a collocated system.

If the state vectors are $x_1 = \eta(t)$ and $x_2 = \dot{\eta}(t)$, then state equations and output equations of the state-space model in vector-matrix form are

$$\begin{bmatrix} \dot{x}_1 \\ \dot{x}_2 \end{bmatrix} = \begin{bmatrix} 0 & I \\ -\Omega^2 & -2 \zeta \Omega \end{bmatrix} \begin{bmatrix} x_1 \\ x_2 \end{bmatrix} + \begin{bmatrix} 0 \\ Q \end{bmatrix} f(t) \quad (2.2a)$$

and

$$w = \begin{bmatrix} Q' & 0 \end{bmatrix} \begin{bmatrix} x_1 \\ x_2 \end{bmatrix} \quad (2.2b)$$

This is similar to the well-known form of the state space:

$$\begin{aligned} \dot{X} &= A X + B F \\ W &= C X \end{aligned}$$

2.2.2 Single-Degree-of-Freedom Floor Model

Considering that the major part of vibration energy is in the first mode, the model of the floor can be approximated by the first mode of vibration, i.e.,

$$\ddot{\eta}_1(t) + 2\zeta_1\omega_1\dot{\eta}_1(t) + \omega_1^2\eta_1(t) = Q_1f(t) \quad (2.3)$$

where the floor response is given by $y(t) = Q_1\eta_1(t)$. Solving $y(t) = Q_1\eta_1(t)$ for $\eta_1(t)$, substituting it into Equation (2.3), and dividing the result by Q_1 yields

$$Q_1^{-2}\ddot{y}(t) + 2\zeta_1\omega_1Q_1^{-2}\dot{y}(t) + \omega_1^2Q_1^{-2}y(t) = f(t) \quad (2.4)$$

This second-order linear-ordinary differential equation resembles the model of a 1-DOF spring-mass-dashpot system (see Equation 2.5), with the parameters of mass $m_f = Q_1^{-2}$, the damping coefficient $c_f = 2\zeta_1\omega_1Q_1^{-2}$, and the spring coefficient $k_f = \omega_1^2Q_1^{-2}$.

$$m_f\ddot{y}(t) + c_f\dot{y}(t) + k_fy(t) = f(t) \quad (2.5)$$

2.3 Floor Excitation and Type of Response

As discussed in the introduction, the floor vibration due to walking in the office environment is transient. This transient response is usually analyzed using a typical test input known as a heel-drop impact [4]. Mathematically, this impact can be approximated

by a decreasing ramp function with a peak of 600 lb. and a duration of 50 ms. [12]. Figure 2.3 shows this ramp-force input. This essential information will be used in chapter 3 to study the transient response of the VPI floor.

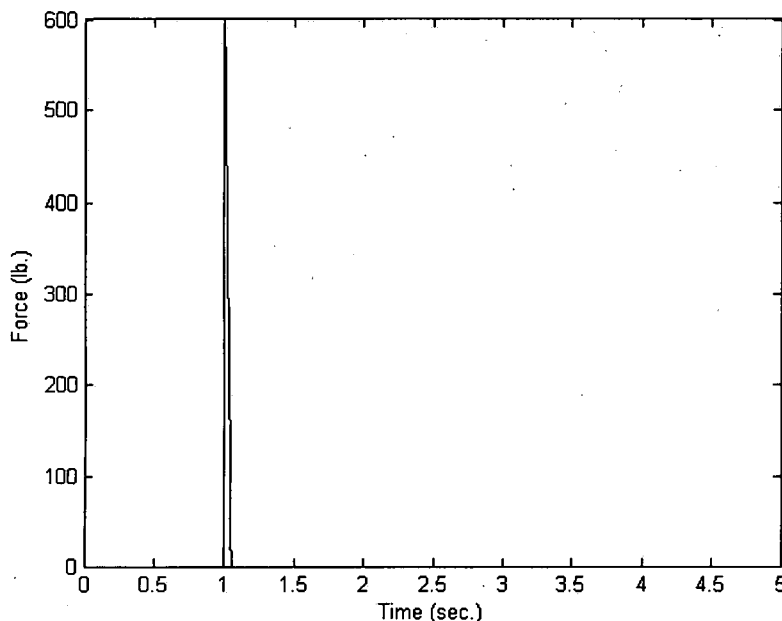


Figure 2.3: Heel-Drop Impact

2.4 Evaluating Floor Vibrations

Both the Murray criterion and the modified Reiher-Meister scale are used to assess the vibration of the VPI floor. Because the VPI floor represents a typical steel- frame office floor and has a first natural frequency that was found earlier to be less than 10 Hz, the Murray criterion, which was discussed in chapter one, is used here to assess its vibration. In this dynamic criterion, a satisfactory floor system should meet the following inequality:

$$D > 35 A_0 f + 2.5 = D_{\text{req'd}}$$

For the VPI floor, Hanagan [5], who was involved in the design of this floor, performed lengthy computations and reported the important parameters for this criterion as follows:

D = Estimated damping of the floor= 1.5%

A_0 =Maximum amplitude of the floor=0.0218 in.

f =Floor fundamental frequency=7.11 Hz

Because the concrete slab of the VPI floor is thin and made of lightweight material and the floor is free of partitions, the floor was estimated to have very low damping ($D=1.5\%$). This very small amount of damping is consistent with the experimental results where the average value of the first five modal damping ratios (Table 2.1) is 0.65%. On the other hand, the required damping for the VPI floor to be satisfactory can be computed as

$$D_{req'd} = 35 A_0 f + 2.5 = 35 (.0218)(7.11) + 2.5 = 7.9\%$$

Because the estimated damping is much less than the required damping ($D \ll D_{req'd}$), the inequality of the Murray criterion is not satisfied. Therefore, the existing VPI floor has an unacceptable level of vibration.

The modified Reiher-Meister scale, which was presented in chapter one, is also used to evaluate the level of vibration of the VPI floor. The fundamental frequency (f) and the maximum amplitude (A_0), which were used in the Murray criterion, are also helpful here for using the modified Reiher-Meister scale. These two vibration parameters (f, A_0) specify a particular point in this scale. Figure 2.4 shows the point ($f = 7.11$ Hz, $A_0 = 0.0218$ in.), denoted by a solid square (■). Because this point is close to the strongly perceptible threshold, it is obvious that the VPI floor has an objectionable motion to the occupants.

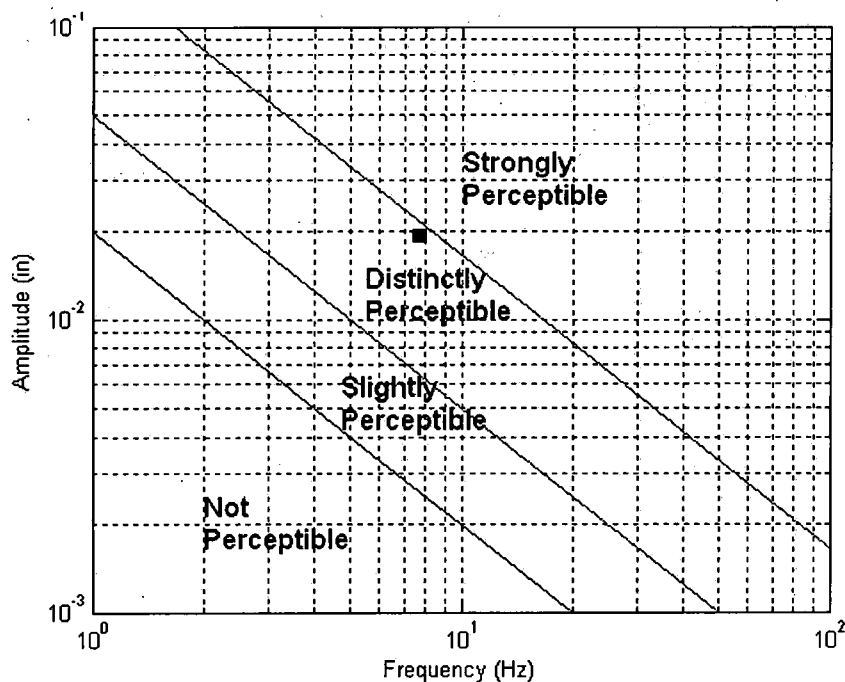


Figure 2.4: Modified Reiher-Meister Scale

Both the Murray criterion and the modified Reiher-Meister scale indicate that the constructed VPI floor needs to be treated. More damping needs to be added artificially to the floor by a passive or an active vibration-control method so that this floor will be satisfactory. This research aims to provide more damping to the VPI floor by a passive TMD.

CHAPTER III

THE USE OF A THREE-DEGREE-OF-FREEDOM TUNED MASS DAMPER TO CONTROL FLOOR VIBRATIONS

A tuned mass damper (TMD), as the name implies, is composed of a mass element, a spring element, and a damping element. The spring element and the damping element, which usually are arranged in parallel, connect the TMD mass to the primary system, such as a structure or a machine. When the TMD is attached to the primary system, part of the primary system's vibrational energy passes to the TMD and dissipates there [19]. Therefore, TMD is a passive energy-dissipation device. When designed correctly, a TMD provides a large amount of damping to the primary system, significantly reducing the excessive vibration of the primary system.

A TMD possesses a single degree of freedom (i.e., it has only one vibration mode); however, the primary system usually has several significant modes of vibration. The TMD is tuned to only one vibration mode, which should be the most significant one of the primary system. As a starting point for analytical vibration analysis, the primary system (i.e., floor) is modeled as a single-degree-of-freedom (SDOF) system that resembles the target mode. Figure 3.1 shows the TMD attached to a SDOF floor model. A clear and precise notation, utilized by Rottmann [6], is used in this research (Figure

3.1). A TMD should be placed at the location of maximum vibration amplitude of the target mode.

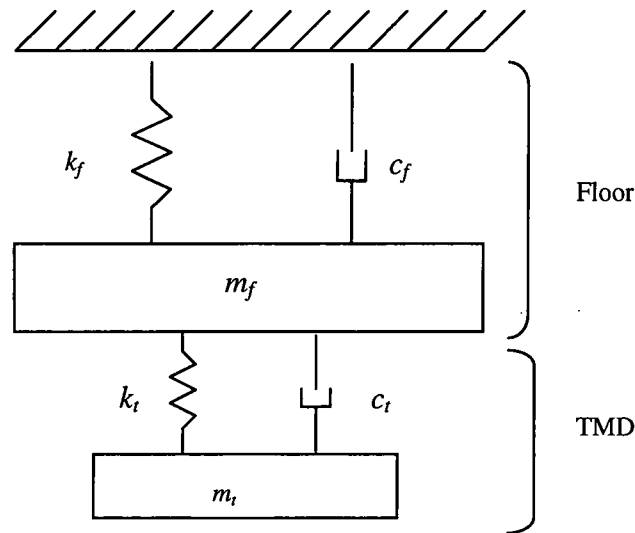


Figure 3.1: A SDOF TMD Attached to a SDOF Floor Model

3.1 Optimal Design of Tuned Mass Damper

Several researchers have tried to enhance the effectiveness of the TMD by increasing its number or degrees of freedom, or by optimizing its parameters. Many have tried to use multiple SDOF TMDs to control many modes of a primary system. Xu and Iqusa [20] have proposed multiple SDOF TMDs to damp one mode. Furthermore, research has shown benefits from optimization of TMD parameters. Zuo and Nayfeh [21] proposed a multi-DOF TMD. They concluded that a multi-DOF TMD is more effective than a SDOF TMD for one mode of a primary system. Den Hartog [22] developed mathematical equations for optimizing SDOF TMD parameters to damp only one mode of an undamped primary system.

An important vibration property of a SDOF system is the natural frequency, which depends on both the mass and the stiffness of the system. This study deals with

two major vibrating systems: the floor and the TMD. Therefore, the natural frequency of the SDOF floor model is

$$\omega_f = \sqrt{\frac{k_f}{m_f}}$$

and the natural frequency of the SDOF TMD is

$$\omega_t = \sqrt{\frac{k_t}{m_t}}$$

where the floor parameters (m_f , k_f) and the TMD parameters (m_t , k_t) are defined in Figure 3.1.

In designing a TMD, it is necessary to determine three variables: the mass ratio μ , the tuning frequency ratio f , and the damping ratio ζ . These three variables (μ , f , ζ), in addition to the knowledge about the primary system parameters (m_f , c_f , k_f), establish the optimal values of the TMD parameters. As mentioned in Chapter 2, the modal parameters (ω_{ni} , Q_i , ζ_i) provide a convenient way to determine the primary system parameters (m_f , c_f , k_f).

The first and most significant design variable is the mass ratio μ . When the modal parameters are used to determine the primary system parameters (m_f , c_f , k_f), the mass ratio is the ratio of the TMD mass to the modal mass of the primary system:

$$\mu = \frac{m_t}{m_f}$$

The mass ratio usually is selected to be within the range of 2% to 7% [6]. When the mass ratio increases, the TMD becomes more effective and robust. Note that the mass ratio does not always depend on the modal mass of the primary system, but instead it occasionally depends upon the actual mass of the primary system. In this work, it is

assumed that the mass ratio involves the modal mass of the primary system, unless otherwise noted.

Next, the tuning frequency ratio f is the ratio of the TMD frequency to the primary system frequency. It can be expressed mathematically as follows:

$$f = \frac{\omega_t}{\omega_f}$$

Finally, the damping ratio ζ is the ratio of damping coefficients to the critical damping coefficient, determined by the following equation:

$$\zeta = \frac{c}{c_c} = \frac{c_t}{2 m_t \omega_t}$$

where m_t and c_t are defined in Figure 3.1. In order to determine the TMD parameters (mass, stiffness, damping), one should first find the proper values of the three design variables (μ , f , ζ). These design variables depend upon the vibration characteristics of the primary system, especially the amount of damping presented in the primary system. In other words, the damping presented in the primary system plays a crucial role in the design of the TMD.

When the primary system is undamped, the two design variables (f , ζ) for a SDOF TMD have closed-form solutions. The simplest scenario occurs when both the primary system and the TMD are undamped. In this special case the TMD, which more appropriately is called a vibration absorber, is a spring-mass system. The frequency of the TMD is simply equal to the target frequency of the primary system (i.e., $f=1$), and the TMD does not have any damping ($\zeta=0$). A dynamic absorber is typically used for controlling the vibration of machines that run at a constant frequency.

Another simple case for using the TMD in the undamped primary system introduces some damping to the TMD. Den Hartage [22] studied this case carefully and developed closed-form solutions for proper values of the tuning frequency ratio and the damping ratio. These two quantities have optimal values and are denoted by f_{opt} and ζ_{opt} , respectively. The optimal tuning frequency ratio is

$$f_{opt} = \frac{\omega_t}{\omega_f} = \frac{1}{1 + \mu}$$

Because the value of the optimal tuning frequency ratio (f_{opt}) usually ranges from 95% to 99% [6], the frequency of the TMD is slightly less than the target frequency of the primary system ($\omega_t < \omega_f$). To introduce reasonable damping to the TMD, the appropriate value of the damping ratio, which is called the optimal damping ratio, needs to be determined. The optimal damping ratio is

$$\zeta_{opt} = \frac{c_t}{2 m_t \omega_t} = \sqrt{\frac{3\mu}{8(1 + \mu)^3}}$$

The optimal ratios (f_{opt} , ζ_{opt}) are both functions of the mass ratio only for the undamped primary system.

For more complex TMD cases, such as a primary system with some damping and a MDOF TMD, the optimal ratios (f_{opt} , ζ_{opt}) do not have closed-form solutions. Warburlon and Yorinde [23] studied the application of TMDs to viscously damped primary systems and listed the optimal ratios. Both the optimal tuning frequency ratio and the optimal damping ratio depend upon the mass ratio and the primary system damping.

Other complex cases involving TMDs can be analyzed individually by using analytical models in advanced software packages, such as MATLAB. These computer packages can easily compute and plot the frequency response for the combined TMD and

primary system. This numerical simulation allows adjustment to the tuning frequency ratio (f) and the damping ratio (ζ) until the optimal values are obtained by having two peaks with reasonable and equal heights.

The values of TMD parameters (m_t , c_t , k_t) depend upon primary system parameters (m_f , c_f , k_f) and the three design variables (μ , f_{opt} , ζ_{opt}). A TMD is more effective with a structure that has very low damping ($\zeta < 3\%$) and has well-spaced natural frequencies (i.e., 2 Hz or more between neighboring frequencies) [6].

3.2 The Proposed Three-Degree-Of-Freedom Tuned Mass Damper

In this work, we have proposed the use of a three-degree-of-freedom tuned mass damper (3-DOF TMD), tuned to one mode, as one effective TMD. The most important attribute of the proposed device is that while its total mass is no more than the mass of an equivalent 1-DOF TMD, it does not require the excessive damping that is needed in a 1-DOF TMD to avoid mode splitting.

The analysis and design of the 3-DOF TMD depends upon the frequency response of the primary system and, eventually, the combined system of the primary system and the attached TMD. As stated earlier, this TMD, like any other TMD, targets only one mode of the MDOF system. The proposed TMD with three degrees of freedom splits the amplitude of the target mode, typically the first mode, into four smaller modes with minimal peaks and minimum energy. Each DOF of the 3-DOF TMD is represented by a unique vibration absorber. The 3-DOF TMD consists of three vibration absorbers² (VAs)

² A vibration absorber can be viewed as a TMD with a very small damping. Theoretically, it is made up of a spring and mass with no damping.

that work together at a single point in the primary system to dissipate the energy provided by external excitations.

The overall proposed system for reducing the vibration is called a 3-DOF TMD, but the three main subsystems (spring-mass subsystems with very small damping) of the 3-DOF TMD are referred to as vibration absorbers (VAs), or simply absorbers. This clarification shall help to distinguish the overall system from the three main subsystems.

One of the unique advantages of using the 3-DOF TMD is its ability to damp the primary system target mode even when its frequency varies slightly. When combined end to end, the three absorbers provide a broad, effective operating frequency range for the 3-DOF TMD. The TMD is most effective when the primary system frequency falls between the frequencies of the second and third absorbers. Here, the first absorber frequency is between the second and third absorber frequencies.

The general procedure for tuning the proposed TMD, which is made up of three vibration absorbers, to a target mode is as follows:

1. Tune the first absorber (in the absence of the other two) to the resonant frequency of the target mode. The low damping attribute of the device allows it to absorb the vibration energy at the tuned frequency and to split the target mode into two neighboring ones, each having a smaller magnitude than the original peak.
2. The other two absorbers are tuned to the newly created two modes (one absorber to one mode). In turn, this will absorb vibration energy at these modes and split them further into four modes with smaller magnitudes.

This process changes the original, highly underdamped target mode, with a large concentration of vibration energy at its resonant frequency, into four neighboring modes with very small energy content.

Different aspects involved in the design of the 3-DOF TMD are illustrated in its application to the full-scale VPI floor. The tuning process of the absorbers, which involves assigning a particular absorber to a specific mode, is described and then demonstrated numerically in a MATLAB simulation. Subsequently, the 3-DOF TMD configuration is defined. Based upon the MATLAB simulation parameters, the new design of the 3-DOF TMD is constructed in ANSYS, and its numerical frequency response is compared to one from MATLAB.

3.3 Design of a 3-DOF TMD to Control Floor Vibration

The modal model of the VPI floor in the state space form, which was developed in Chapter 2, is used here in MATLAB to simulate the vibration at the center of the floor. The frequency response function (FRF) of the untreated floor, measured at the center of the floor, shows three distinct resonant frequencies (7.3, 16.9, and 26.5 Hz), indicated by the three sharp peaks (see Figure 3.2). These three dominant modes correspond to the first, fourth and fifth modes. The second and third modes are not shown in Figure 3.2 because their nodes (zero deflections) are at the center of the floor.

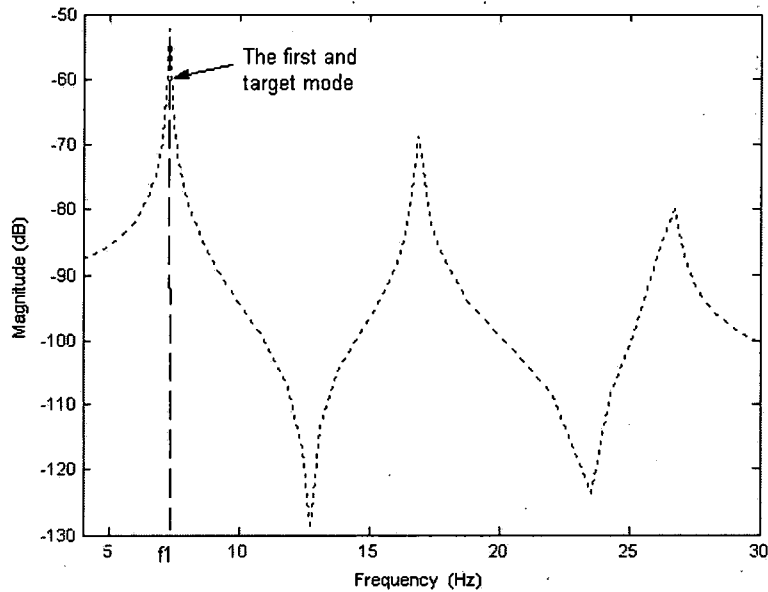


Figure 3.2: Magnitude of the FRFs' Mapping Force to the Displacement at the Center of the Floor

In order to control vibration of the VPI floor, at least one of the dominant modes of vibration needs to be treated. It is obvious that the fundamental mode, which has the first sharp peak in Figure 3.2, has more energy than any other mode. This mode also has very low damping ($\zeta_1=0.5\%$) and is well spaced from the second mode (more than 2 Hz between them). Due to these characteristics, an inadequate amount of damping causes excessive floor vibration, which is predicted, using the criteria discussed in Chapter 2, to be very annoying to the occupants. From the calculations of the Murray criterion's parameters (computed in Chapter 2), the required damping ($D_{req'd}$) for this floor was 7.9%. To meet this damping requirement, additional damping needs to be provided properly to the first mode of vibration. A promising solution to this floor-vibration problem is the application of the TMD to the floor model. A single 3-DOF TMD is used to control the fundamental mode of vibration of the VPI floor model. It is placed at the

center of the floor model where the antinode (maximum amplitude) of the first mode is located.

Before determining the exact values of the three absorbers' parameters (m_{ii} , k_{ii} , c_{ii} , $i=1,2,3$), it is important to specify three general design variables: mass ratio (μ_i), damping ratio (ζ_i), and optimal tuning frequency ratio (f_{opti}). The mass ratio of the 3-DOF TMD is selected to be $\mu=5\%$. Because this TMD has three degrees of freedom, which are represented by the three absorbers, this mass ratio is divided by three, resulting in a mass ratio of $\mu_i=1.67\%$ for an individual absorber. Every absorber has a very low damping ratio of only 3%. Unlike the mass ratio and the damping ratio, which have the same values for all of the absorbers, the third design variable, the optimal tuning frequency ratio, has a distinct value for each absorber. The optimal tuning frequency ratio varies in range from 0.92 to 1.01. Its exact value for each absorber can be obtained by fine tuning each absorber until the frequency response magnitude of the combined system has two peaks with equal heights.

After describing both the floor-system parameters (first mode with Equation 2.5) and the three design variables (μ_i , f_{opti} , ζ_i), what remains is to define the parameters of the three absorbers. The 3-DOF TMD has three absorbers, each one and its parameters denoted by a unique subscript i , where i is an integer and is in the range from 1 to 3. For example, the i^{th} vibration absorber is denoted by $V A_i$ and has the parameters (m_i, c_i, k_i). To obtain the optimal parameters for each absorber, Equations (3.1) through (3.4) should be used.

The TMD frequency is

$$\omega_{ii} = \sqrt{\frac{k_{ii}}{m_{ii}}} \quad (3.1)$$

the mass ratio is

$$\mu_i = \frac{m_{ii}}{m_f} \quad (3.2)$$

the optimal tuning frequency ratio is

$$f_{opti} = \frac{\omega_{ii}}{\omega_f} \quad (3.3)$$

and the damping ratio is

$$\zeta_{ii} = \frac{c_{ii}}{2 m_{ii} \omega_{ii}} \quad (3.4)$$

Figure 3.3 depicts the block diagram of the three absorbers (VA1 to VA3) appended to the floor. The block diagram holds the functional relationship between the state-space model of the floor and the transfer functions of the three absorbers [24, 25]. This block diagram in a MATLAB/SIMULINK environment provides the basis for numerical simulation of the system in a convenient way.

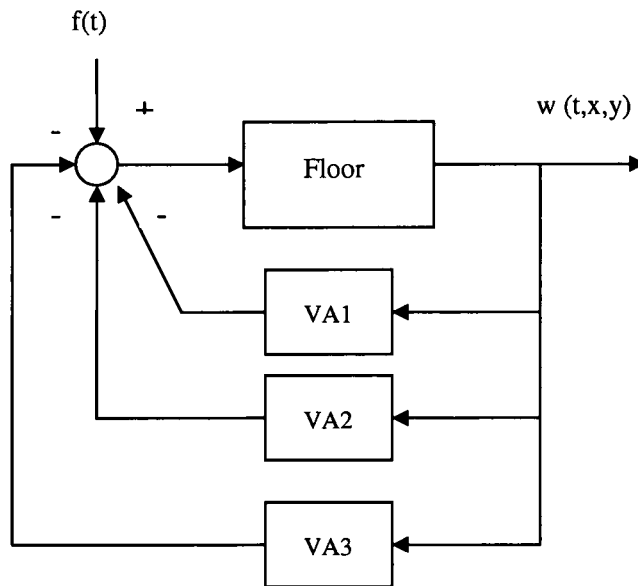


Figure 3.3: Simulation block diagram

For each DOF of the 3-DOF TMD, a unique vibration absorber is assigned to eliminate a specific resonant peak at a particular resonant frequency. When only the first DOF is added to the floor by the first absorber (VA1) and is tuned to the first resonant

peak of the floor, the first floor peak at the first resonant frequency ($f_1=7.3$ Hz) is abated. The combined system of the floor and the first absorber generate two new resonant peaks at two new resonant frequencies, $f_{11}=6.82$ Hz and $f_{12}=7.72$ Hz. One of the new frequencies (f_{11}) is less than the floor fundamental frequency ($f_{11}<f_1$), while the second frequency (f_{12}) is greater than the floor fundamental frequency ($f_{12}>f_1$). At this point, there is a need to abate the newly generated two resonant peaks (f_{11} and f_{12}). This is done by involving the remaining two DOFs of the TMD with the addition of the other two absorbers, VA2 and VA3. The second absorber (VA2) is tuned to the first new resonant peak at $f_{11}=6.82$ Hz, and the third absorber (VA3) is tuned to the second new resonant peak at $f_{12}=7.72$ Hz. As a result, the composite system of the floor and the 3-DOF TMD absorbers has four new, smaller resonant peaks at four new resonant frequencies (see Figure 3.4). Because the four new peaks have almost equal heights at the four new closely spaced resonant frequencies, the 3-DOF TMD is optimally tuned. Introduction of a small amount of damping into the three tuned absorbers will further lower the peaks in magnitude (and thus dissipate energy) at the newly created frequencies, enhancing the effectiveness of the proposed 3-DOF TMD.

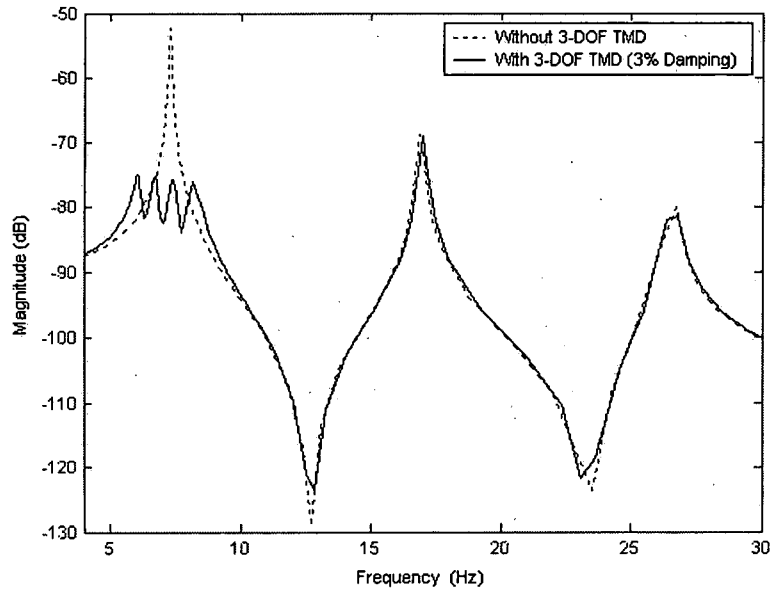


Figure 3.4: Magnitude of the FRFs' Mapping Force to the Displacement at the Center of the Floor

Figure 3.4 shows the magnitude of two frequency response functions of the floor with and without the 3-DOF TMD tuned to the first mode. As shown in Figure 3.4, the proposed TMD has effectively added damping to the first mode, thereby eliminating the first sharp peak. By attaching the 3-DOF TMD to the floor, the equivalent viscous damping ratio of the first mode increases from 0.5% to about 7.5%. This relatively high new damping (7.5%) is very close to the required damping ($D_{req'd}=7.9\%$), which was computed by the Murray criterion previously in Chapter 2.

Optimal values of the 3-DOF TMD parameters are obtained by using the numerical simulation with the proper tuning process. The parameters of the 3-DOF TMD tuned to the first mode of the VPI floor are listed in Table 3.1. This table contains the parameters of the three absorbers. For each absorber, the target and absorber frequencies (ω_n , ω_i), the three design variables (μ_i , f_{opti} , ζ_i), and the absorber parameters (m_{ti} , k_{ti} , c_{ti}) are specified.

Table 3.1: Simulation Parameters

Absorber Parameters		VA1	VA2	VA3
ω_{ni}	rad/s	45.87	42.7	49.1
f_{opti}	-	.96	.925	1
ω_{ti}	rad/s	44.03	39.50	49.1
μ_i	%	1.67	1.67	1.67
ζ_i	%	3	3	3
m_{ti}	lb. s ² /in	3242.27x10 ⁻⁴	3242.27x10 ⁻⁴	3242.27x10 ⁻⁴
k_{ti}	lb/in	628.63	505.81	781.65
c_{ti}	lb. s/in	8565.92x10 ⁻⁴	7683.68x10 ⁻⁴	9551.71x10 ⁻⁴

The first absorber frequency falls between the second absorber frequency and the third absorber frequency ($\omega_{t2} < \omega_{t1} < \omega_{t3}$). Because the value of the first absorber frequency is approximately equal to the average of the other two absorbers' frequencies, the first absorber is referred to as the center absorber. Indeed, the frequencies of the other two absorbers are spaced closely to the frequency of the center absorber. Because the frequency of the second absorber is slightly less than the frequency of the first absorber, the values of the second absorber parameters are either equal to or slightly less than the values of the first absorber parameters. Similarly, the values of the third absorber parameters are either equal to or slightly greater than the values of the first absorber parameters because the frequency of the third absorber is slightly greater than the frequency of the first absorber.

Because the values of each absorber parameters are either identical or very close to the values of the other absorber parameters, the parameters of one absorber can provide an accurate general approximation. Finding the optimal values of the center absorber parameters is of primary concern. Therefore, determination of the center

absorber (VA1) parameters is essential. The parameters of the other two absorbers are less important, especially considering that the three absorbers have closely spaced natural frequencies and identical masses.

It is important to analyze the transient response of the VPI floor without and with the attached 3-DOF TMD. The heel-drop impact, which was defined in Chapter 2, is applied at the center of the floor and subsequently the floor response is evaluated. The 3-DOF TMD, with only five percent of the floor's first modal mass ($\mu=5\%$), has the ability to reduce the amplitude of the floor's transient vibration to less than 20% in just three cycles (see Figure 3.5). Only 3% damping in each absorber is sufficient to yield effective vibration abatement. For more vibration reduction, either the mass ratio (μ) needs to be increased or more than one of a 3-DOF TMD should be used. Similar to frequency response, a definite improvement in the floor time response is achieved.

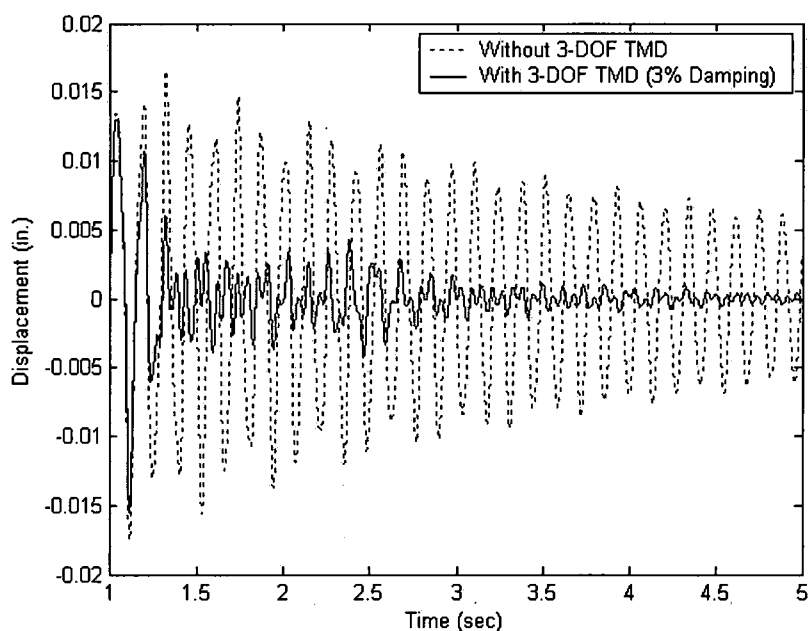


Figure 3.5: Transient Response at the Center of the Floor to a Heel-Drop Impact

Both the damping amount and the frequency of the dominant vibration mode have a strong effect on the perception and comfort of the occupants. From the information presented in Chapter 1, it is obvious that the human body is sensitive to vibration, especially within the frequency range of 5 to 8 Hz. Figure 3.5 shows that the floor without the 3-DOF TMD vibrates at the first natural frequency, 7.3 Hz. This results in floor motion that can be very distracting to the occupants. However, Figure 3.5 demonstrates that the floor with the 3-DOF TMD vibrates with lower amplitude at higher frequencies, limiting the vibration that is felt by the occupants. The vibration amplitude of the floor without the 3-DOF TMD after five cycles of vibration is more than forty percent of the initial amplitude. Lenzen [10] classifies this floor oscillation as being definitely perceptible. In contrast, the vibration of the floor with the 3-DOF TMD would be categorized, according to Lenzen [10], as being barely perceptible or not perceptible at all because the amplitude of vibration after five cycles is less than twenty percent of the initial amplitude.

3.3.1 The Configuration of the 3-DOF TMD

The 3-DOF TMD has a unique configuration. To implement the proposed 3-DOF TMD in a convenient way that is practical and yet inexpensive, the 3-DOF TMD design uses three cantilevered beams with end masses for the three absorbers as shown in Figure 3.6. That is, each absorber is composed of a uniform cantilevered beam and a concentrated mass at the free end. For convenience, the three beams should be made from the same material and should have the same cross sections. The three beams lie on a horizontal plane, and the angle between any two of them is 120° . A small amount of damping must

be introduced properly to every absorber. Information on the different forms of damping will be presented later in this chapter.

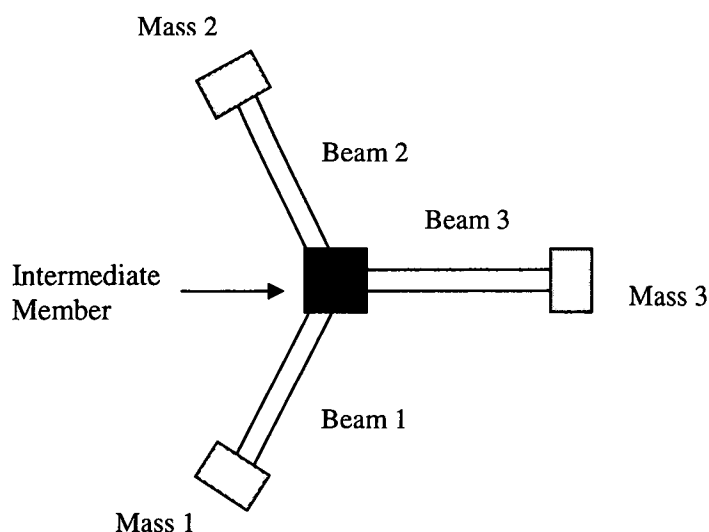


Figure 3.6: The 3-DOF TMD

A rigid intermediate member should be introduced, as shown in Figure 3.6, to connect the 3-DOF TMD properly to the floor. This intermediate member supports the 3-DOF TMD, which lies in a single horizontal plane parallel to the floor horizontal plane. As a result, the intermediate member is perpendicular to the floor plane and the 3-DOF TMD plane. This intermediate member should be stiff and small enough not to introduce its own dynamics into the three absorbers. However, it should have enough height to allow the masses at the tips of the three beams to vibrate freely without striking the floor. In other words, the height of the intermediate member should be greater than the amplitudes of the vibrating beams. It is important that the intermediate member has a sufficient area at the top for attaching the roots of the three beams. The intermediate member that can provide the necessary geometric shape (i.e., enough height with

sufficient area at the top) with the minimum weight could be a structural element with hollow cross sections, such as tubes.

In our work, the intermediate member is chosen to be a square tube that rests in a horizontal position. This shape gives enough height and provides sufficient top area (in this case, the upper wall) for installing the three absorbers. Moreover, it has a beneficial light weight. The square tube is placed on the center of the top surface of the floor model. The lower wall of the square tube is joined to the floor. The steel, square tube has outside dimensions of 6 inches by 6 inches and a wall thickness of 1 inch.

A concentrated mass at the tip of a cantilevered beam can cause a dramatic change in the dynamic behavior of the beam. A cantilevered beam is a continuous system with infinite degrees of freedom; but if a considerable mass is added to the tip of the beam, the beam behaves as a spring, and the beam with the end mass acts as a spring-mass system with a single degree of freedom. The end mass must be large when compared to the mass of the beam. That is, the mass at the tip of the beam is at least approximately 1.5 times as large as the mass of the beam so that the cantilevered beam with end mass starts to function as a spring-mass system.

The three absorbers' parameters (m_t and k_t) can be characterized in terms of geometric properties (i.e., area moment of inertia I and beam length L) and material properties (elastic modulus E and beam mass m) for the three uniform beams and their end masses ($M1$, $M2$, $M3$). At low frequencies, a cantilevered beam of mass (m) supporting an end mass (M) can be viewed as a spring-mass system, with the equivalent mass (m_t) and stiffness (k_t) defined by Equations 3.5 and 3.6 (see Figure 3.7).

$$m_t = M + \frac{33}{140} m \quad (3.5)$$

$$k_t = \frac{3EI}{L^3} \quad (3.6)$$

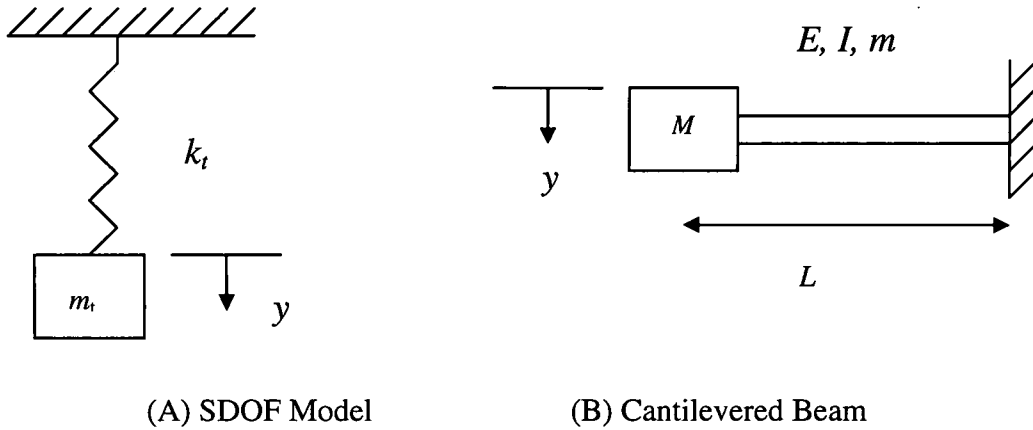


Figure 3.7: Equivalent Spring and Mass

Note that the flexibility of the cantilevered beam represents the stiffness in the spring [11]. The flexibility of the beam, in turn, relies upon both the geometric dimensions and the material of the beam. The entire mass at the tip of the beam and a portion of the mass of the beam represent the mass element in the spring-mass system.

Because the end mass must be considerably larger than the beam mass ($M > m$) and only about one-fourth of the beam mass (m) is considered in the equivalent mass of Equation 3.5, the beam mass (m) is neglected in this equation. As a result, the equivalent mass is approximately equal to the end mass ($m_t \approx M$). This is consistent with most of the analytical work in dynamics where the spring, which in this case is the beam, is assumed to be massless. This simplifies the computation of the equivalent mass for the three absorbers and considers the three beams to have equal end masses, a shortcut in finding the frequency. As a result, the frequency of the transverse vibration of the mass at the tip of the beam simply becomes

$$\omega_n = \sqrt{\frac{k_t}{m_t}} = \sqrt{\left(\frac{3EI}{L^3}\right)\left(\frac{1}{M}\right)}$$

Similar to the numerical simulation where the absorber is tuned optimally to the target mode by the optimal value of the tuning frequency ratio f_{opti} (i.e., $\omega_t = f_{opti} \omega_f$), the physical tuning process requires at least one parameter of the absorber, such as mass or stiffness, to vary. Tuning of the three absorbers of the 3-DOF TMD is achieved by modifying the stiffness while the mass and the damping remain the same [6]. The only variable factor in the stiffness of the beam with end mass is the beam length. An adjustment to the length of the beam is needed until the stiffness reaches the desired value. Because the three absorbers are tuned to three distinct modes, the three beams of the three absorbers have different lengths. Among the mass and stiffness parameters (M , E , I , L), only the length is computed exponentially (i.e., raised to the third power). Therefore, a slight change in length produces a considerable variation in the frequency.

Later in the experimental work (chapter 5), the design of each absorber will be improved further. Specifically, a short, narrow, rectangular slot is created near the tip of the beam to easily change the effective length of the beam. The concentrated mass is then able to slide easily until the absorber is tuned properly.

3.3.2 The Finite-Element Analysis

ANSYS, as a design tool, is used to predict the effectiveness of the 3-DOF TMD before that TMD is physically built and examined in the laboratory. This allows for modifications and improvements to the proposed TMD system design. This design of the 3-DOF TMD is modeled in ANSYS, similar to the VPI floor in chapter 2. In the finite-element model of this new TMD, beam elements are used for the three beams, shell

elements are used for the walls of the square tube, and mass elements are used for the three end masses.

To continue developing the finite-element model of a 3-DOF TMD after defining its configuration, both the materials and the dimensions of its three beams need to be specified. Steel is a frequently used metal that is known to be elastic and can be used for making the three springs (i.e., the three beams). The three beams are made of steel (Structural A36) with $E=29 \times 10^3$ ksi. A very important step in designing the 3-DOF TMD is to choose the proper dimensions for the cross sections of the three beams. Because the three beams carry the same concentrated load at their tips, they should have the same cross sections. A beam with the least amount of material should be chosen so that the beam can be light and less expensive. For simplicity, every beam has a rectangular cross-sectional shape with a width (b) of 2 inches and a height (h) of 0.75 inches.

The values of the three absorbers' parameters (m_{ti} , c_{ti} , k_{ti} , where $i=1,2,3$) are available from the numerical simulation (Table 3.1). Even though these simulation parameters depend upon the floor modal model that was provided by modal parameters (not only from the finite-element method but also from experimental modal analysis), they are still valid here because the experimental data, especially the natural frequency, is very close to the finite-element data.

On the other hand, the material and the cross-sectional dimensions of the three beams are known. As a result, both the equivalent stiffness equation (3.6) and the approximate equivalent-mass equation (i.e., $m_t=M$) are used to determine the tip mass and length of each beam. The mass at the tip of each beam is 3242.27×10^{-4} lb.s²/in.

(equivalent to approximately 123.1 lbs.). Here, the tip mass is directly related to the first modal mass and the mode shape of the floor (i.e., $M=m_t=\mu m_f = \mu Q_1^{-2}$). Table 3.2 lists the tip masses and the geometric properties of the three beams.

Table 3.2: Initial Design Parameters of the 3-DOF TMD

Geometric and Material Properties		VA1	VA2	VA3
M	(lb.s ²)/in.	3242.27×10^{-4}	3242.27×10^{-4}	3242.27×10^{-4}
b	in.	2	2	2
h	in.	0.75	0.75	0.75
I	in. ⁴	70.31×10^{-3}	70.31×10^{-3}	70.31×10^{-3}
L	in.	21.35	22.95	19.85

Table 3.2 shows various similarities between the three absorbers. The three beams have identical cross sections and end masses. Because the three beams have identical cross sections, they are of equal width b , height h , and area moment of inertia I . The frequencies of the three absorbers are spaced closely (about 0.75 Hz difference between each frequency and the adjacent one); therefore, the three beams are very close in length. More precisely, the first beam's length is slightly shorter than the second beam's length ($L_1 < L_2$), and the third beam's length is slightly shorter than the first beam's length ($L_3 < L_1$); thus, the differences in lengths can be summarized as $L_3 < L_1 < L_2$.

The finite-element model of the 3-DOF TMD is attached to the finite-element floor model discussed earlier in Chapter 2. Because the square tube is assumed to be joined to the floor by four bolts near the corners of its lower wall, both the finite-element mesh of the floor and the finite-element mesh of the square tube's lower wall should have four coincident nodes at the approximate locations of the four joining bolts. The mesh size for the slab is reduced from 30 inches x 30 inches to 3 inches x 3 inches in order to

allow the finite-element meshes for the floor and the square tube to have four coincident nodes at the approximate locations of the four bolts. In addition, the mesh size for the square tube is selected to be 1 inch x 1 inch. The six degrees of freedom of coincident nodes for both the square tube and the floor at the approximate locations of these bolts are coupled. Unfortunately, this finite-element mesh produces 6000 elements for the concrete slab alone. This incredible number of elements is impractical, especially for the harmonic analysis, where the computations of the matrices are lengthy and need a lot of time for the 30-Hz frequency range.

Another approach for modeling the combined system in the ANSYS is considered. In this approach, the mesh size of the walls of the square tube is 1 inch by 1 inch. With the mesh size for the floor equal to 30 inches x 30 inches, the floor has only two nodes below the square tube. These two nodes are located at the geometric center of the floor. One of these two nodes is related to the center joist, and the other is related to the concrete slab. These nodes at the center of the floor are coincident with a third node from the center of the lower wall of the square tube. The six degrees of freedom of these coincident nodes are coupled because the lower wall of the square tube is fixed to the floor. In order to prevent the rotation of the square tube around a vertical axis passing through the center of the lower wall, two degrees of freedom (translations in x and y directions) of two nodes at the sides of the lower wall are coupled to the corresponding degrees of freedom of the nodes at the center of the floor. Each beam is divided into forty-three elements (mesh size of about 0.5 inches). This finite-element approach leads to positive numerical results. The finite-element mesh for the floor model, the square tube, and the 3-DOF TMD without damping mechanisms is shown in Figure 3.8.

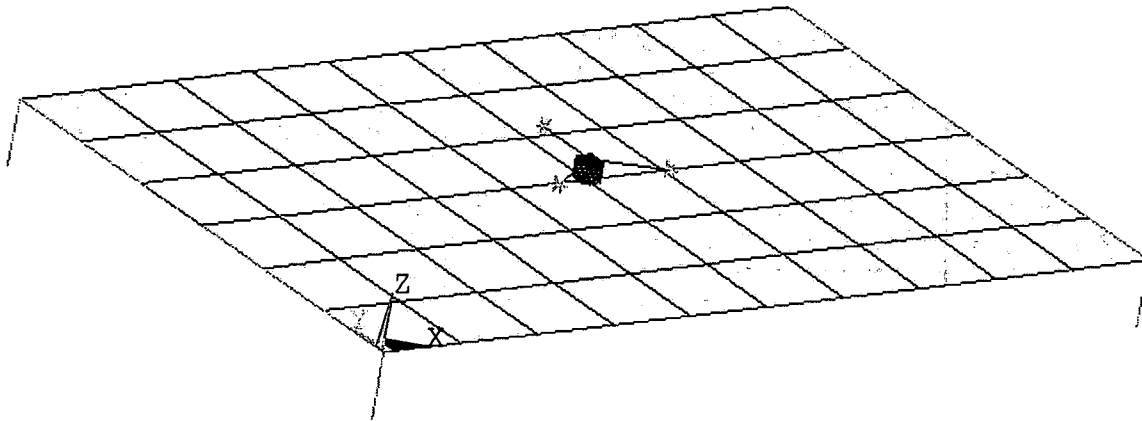


Figure 3.8: The Finite-Element Mesh of the Floor With the 3-DOF TMD

Harmonic analysis of the combined system of the floor and the 3-DOF TMD without damping treatment, subject to the same forcing function as used in Figure 3.2, results in the frequency response in Figure 3.9. This frequency response is similar to the frequency response of Figure 3.4, but the four new peaks of the finite-element model are sharper because no damping has been introduced to the three absorbers. The measured frequency response function with and without the 3-DOF TMD shows that the 3-DOF TMD is very effective in breaking the first mode into four new smaller, closely spaced peaks.

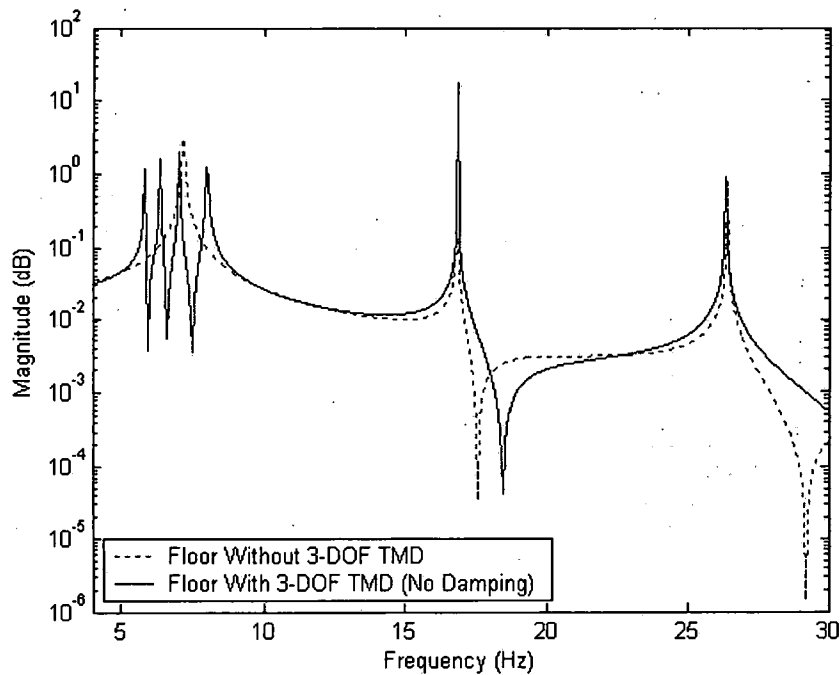


Figure 3.9: The Frequency Response of the Floor With and Without the 3-DOF TMD (No Damping)

As was stated earlier, a small amount of damping must be introduced into the three dynamic vibration absorbers in order to lower the four new peaks in magnitude and to increase the effectiveness of the proposed 3-DOF TMD. Figure 3.10 shows the frequency response magnitude of the floor and the 3-DOF TMD with and without 1% damping in each absorber. This very small amount of damping in each absorber produces a significant reduction in the magnitude of the four new resonant peaks. The presence of damping enhances the effective bandwidth of the absorber [26, 13]. As a result, the resonant vibration is attenuated.

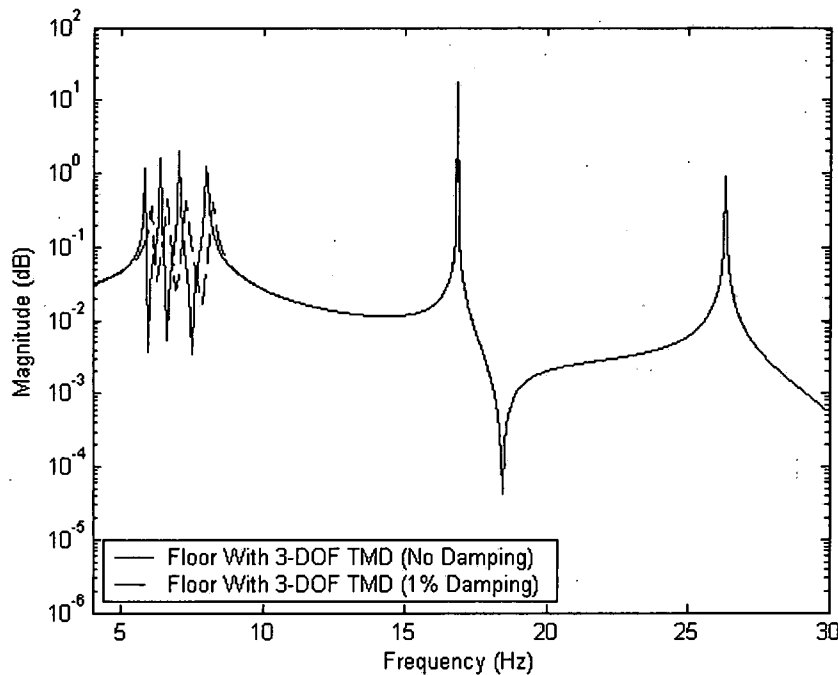


Figure 3.10: The Frequency Response of the Combined System With and Without 1% Damping in Each Absorber

The proposed 3-DOF TMD has several advantages over the typical TMD. First, the 3-DOF TMD does not need helical springs and viscous dashpots, which might not fit in the joist cavity of some floors. Additionally, it does not require one location, like the typical TMD with a large mass, spring, and dashpot. That is, the 3-DOF TMD can be expanded on a plane. Moreover, the size of the 3-DOF TMD is somewhat flexible. The moment of inertia (I) of the beam's cross section can be varied until the appropriate beam length (L) is achieved. As a result, this 3-DOF TMD can be sized such that it can be installed in the ceiling cavity, connected to the upper chord of the center joist. Finally, the 3-DOF TMD seems to be less costly than the typical TMD.

3.4 Introduction of Damping to the Absorbers

The amount of damping presented in each absorber has a strong influence on both the absorbers and the overall effectiveness of the 3-DOF TMD. An inadequate amount of damping for each absorber ($\zeta_i < 3\%$, $i=1,2,3$) causes the 3-DOF TMD to be less effective, but a very modest amount of damping ($3\% \leq \zeta_i \leq 6\%$, $i=1,2,3$) results in an effective system. An absorber with a cantilevered beam that is constructed from one layer (strip) and is made from metal (e.g., steel or aluminum) naturally has a very low damping ($0 < \zeta \leq 2\%$); therefore, it is important to provide the necessary artificial damping to each absorber. Every absorber is like any spring-mass-damper system. As a consequence, it can have one of different forms of damping. Unlike the typical spring-mass-damper system or TMD, which commonly requires a large amount of viscous damping, every absorber in the 3-DOF TMD needs only a small amount of damping. Thus, the damping can be introduced into the three beams through two different approaches of coulomb damping and viscoelastic damping. In both approaches, there is a special design for the cantilevered beams with end masses.

The first approach to add more damping to the three absorbers is coulomb damping. Dry friction between the sliding surfaces results in coulomb damping [27]. In this approach, each cantilevered beam is constructed from two identical metal strips that are bolted together along their length to create the sliding surfaces along the beam. Frictional (damping) force depends upon the contact (joining) force and the nature of the sliding surfaces. If fasteners (bolts), which represent the source of the contact force, are tight, the two strips come in contact along their length. When the beam vibrates, the strips are deflected repeatedly and slide relative to each other. If the two strips have smooth

surfaces, they produce little friction when they are rubbed against each other. Smooth contacting surfaces should be sanded, with sandpaper, in order to create rough surfaces and obtain adequate friction. When the two strips with treated surfaces are rubbed together rapidly while they are vibrating, the friction produces sufficient damping. This simple type of damping exists internally in the vibrating beam. On the other hand, when these bolts are very tight, the strips are bonded together and the sliding between contacting surfaces is minimal. Even though the damping in the two-layer beam is due mainly to friction between the two surfaces, the oscillating beam still has many other forms of damping, including friction at the joints and material damping.

The other approach for providing more damping to the three vibrating beams is to add viscoelastic material to the beams. Viscoelastic material, such as rubber and nylon, has a great ability to dissipate the vibrational energy of a lightly damped system [27]. There are two basic ways for adding viscoelastic material to a cantilevered beam. One arrangement is known as unconstrained-layer damping. This procedure adds damping tape or an adhesive layer to the surface of an existing beam. However, a more effective way is to design the beam specially so that a layer of viscoelastic material is compressed between the two metal strips [27]. This arrangement for the damping layer is known as a constrained-layer damping and is shown in Figure 3.11. Due to the shear deformation of the middle viscoelastic layer, the viscoelastic material dissipates energy. This causes the sandwich-beam system to provide a sufficient amount of damping. This damping material not only increases the amount of damping present in the new system; it also slightly increases its stiffness. The amount of damping provided by this particular material depends upon both the operating temperature and the frequency. Care should be taken to

choose the appropriate viscoelastic damping material for the operating frequency and the environment's temperature. In this design the viscoelastic polymer SJ2015 Type T1210, manufactured by 3M with the thickness of 10 mil., was used.

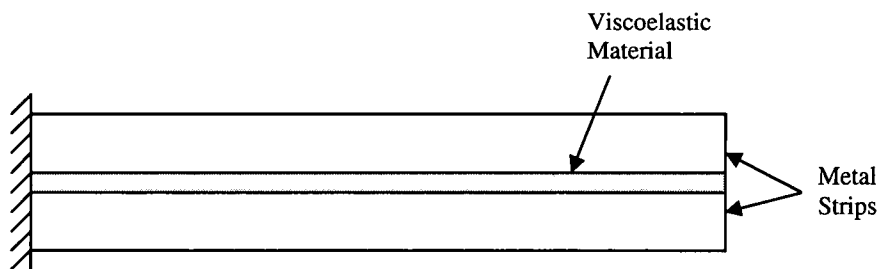


Figure 3.11: A Constrained-Layer Damping

CHAPTER IV

BUILDING A SCALE MODEL OF THE FLOOR

In this chapter, the development of a scale model of the VPI floor is discussed. The purpose of this laboratory scale model is to verify the effectiveness of the proposed floor-damping mechanism. This model, which represents the dynamic behavior of the actual floor, has vibration characteristics that are as similar as possible to those of the actual VPI floor. This chapter describes the design and the construction of a scale model of the VPI floor.

Because the VPI floor is large and the available laboratory space is limited, we need to scale the floor model down to the appropriate size. The floor model does not need to be made of the same materials as those of the actual floor (i.e., steel and concrete). The most important step in building a scale model of the floor is developing a method for scaling down the actual floor into one that is reasonably sized and, for convenience, made of a single material. The scaling factor for this model is chosen to be $1/6$.

Several assumptions are required for scaling down the VPI floor. First, we assume that the material, which is homogenous and anisotropic, behaves in a linear, elastic fashion. Another necessary assumption is to neglect the distributed loads on the structural

members so that the closed-form solutions of the natural frequencies and mode shapes can exist. Finally, it is expected that the boundary conditions in the scale model are identical to the boundary conditions in the actual floor.

In the search for a proper floor scale model that has the desired vibration characteristics, two scale models of the VPI floor are developed. The first is made of engineered wood. Because it has a large amount of internal damping, a model made of steel is also considered.

In the scaling process, the important vibration parameters are the modal parameters (i.e., natural frequencies, mode shapes, and damping ratios). Both the natural frequencies and the mode shapes are considered in the analytical scaling procedure. Damping is not considered analytically in the scaling process because it is not easy to model mathematically. At the end of this chapter, more details will be given about the damping of the scale model.

4.1 The Wooden Scale Model of the VPI Floor

4.1.1 An Initial Scale Model of the Floor

A complex structure like the VPI floor has three types of structural members: the beam (girder and joist), the plate (the composite of the concrete slab and the metal deck), and the column. To scale down the floor, scaling of each structural component is needed. In the wooden scale model, the entire model of the floor is made of tempered hardboard.

4.1.1.1 Beam Scaling

In scaling a beam, it is important to consider two modal properties: the natural frequencies and the mode shapes. The natural frequencies for the transverse vibration of a uniform, scaled-down wooden-beam model with pinned-pinned end conditions can be written as

$$\omega_{scaled}^r = (r\pi)^2 \sqrt{\frac{E_w I_{sc}}{\rho_w A_{sc} L_{sc}^4}} \quad r=1,2,\dots \quad (4.1)$$

It is clear that the frequency of a scaled-down beam model depends on both the material property of wood (E_w and ρ_w) and the scaled-down geometric properties (I_{sc} , A_{sc} and L_{sc}). Because the structural dynamics of the beam are a function of both material and geometry, the scaling-down procedure is lengthy and involves a series of algebraic steps when there is a change in both the material and the geometry of the beam.

It is convenient to define the following relations for scaling down the geometry of the beam model,

$$L_{sc} = G_L L_{real} = \text{Length of the scaled-down beam}$$

$$I_{sc} = G_I I_{real} = \text{Moment of inertia of the scaled-down beam}$$

$$A_{sc} = G_A A_{real} = \text{Cross-sectional area of the scaled-down beam}$$

where G_A and G_I are the area- and the moment-of-inertia modifying factors. G_L is the scaling factor of the beam's length. G_A and G_I primarily modify the beam model's cross section according to the scaling factor G_L . More precise equations will be given shortly.

The following ratios relate the material property of the beam model (E_w and ρ_w), which is made of wood, to the material property of the real beam (E_{st} and ρ_{st}), which is made of steel,

$$M_{Eb} = \frac{E_w}{E_{st}} = \text{Modulus of elasticity ratio}$$

$$M_{\rho b} = \frac{\rho_w}{\rho_{st}} = \text{Density ratio}$$

where E_w and ρ_w are the modulus of elasticity and the mass density of the scale model of the beam, respectively. E_{st} and ρ_{st} are the modulus of elasticity and the mass density of the actual beam, respectively. Both M_{Eb} and $M_{\rho b}$ determine the changes in the material property of the system. The second subscript b in the material ratios (M_{Eb} , $M_{\rho b}$) refers to the beam.

The beam model's natural frequencies, as given in Equation (4.1), can be expressed now in terms of the real beam's frequencies and the previously defined geometric factors and material ratios

$$\omega_{scaled}^r = \sqrt{\frac{M_{Eb} G_I}{M_{\rho b} G_A G_L^4}} (r\pi)^2 \sqrt{\frac{E_{st} I_{real}}{\rho_{st} A_{real} L_{real}^4}} = F_B \omega_{real}^r \quad r=1,2,\dots \quad (4.2)$$

where F_B is the beam frequency factor defined by Equation (4.3)

$$F_B = \sqrt{\frac{M_{Eb} G_I}{M_{\rho b} G_A G_L^4}} \quad (4.3)$$

Solving Equation (4.3) for G_I yields

$$G_I = \frac{G_A M_{\rho b} F_B^2 G_L^4}{M_{Eb}} \quad (4.4)$$

The moment-of-inertia modifying factor G_I depends upon the changes in the material, the geometry, and the frequency from the actual floor structure to the model. It is often preferable for the beam frequency factor F_B to equal one so that the actual beam and the beam model can have identical natural frequencies. The scaling factor G_L of the

beam's length has a substantial influence on the value of the moment-of-inertia modifying factor G_I because it is raised to the fourth power.

Another important vibration characteristic that needs to be considered for the beam model is the mode shape. The mode shapes of the scaled-down wooden-beam model can be written as

$$W_{scaled}^r = \sqrt{\frac{2}{\rho_w A_{sc} L_{sc}}} \sin\left(\frac{r\pi x_{sc}}{L_{sc}}\right) \quad r=1,2,\dots \quad (4.5)$$

Similar to the frequencies, the mode shapes of the scaled-down beam model depend upon the material and the geometry. The scaled-down beam's mode shapes, as given in Equation (4.5), can be expressed now in terms of the real beam's mode shapes and the previously defined geometric factors and material ratios

$$W_{scaled}^r = \sqrt{\frac{1}{M_{pb} G_A G_L}} \sqrt{\frac{2}{\rho_{st} A_{real} L_{real}}} \sin\left(\frac{r\pi x_{real}}{L_{real}}\right) = S_B W_{real}^r \quad r=1,2,\dots \quad (4.6)$$

where S_B is the beam mode-shape factor defined by Equation (4.7)

$$S_B = \sqrt{\frac{1}{M_{pb} G_A G_L}} \quad (4.7)$$

Solving Equation (4.7) for G_A yields

$$G_A = \frac{1}{G_L M_{pb} S_B^2} \quad (4.8)$$

The area-modifying factor G_A depends upon the scaling factor of the beam's length, the density ratio, and the square of the beam mode-shape factor. As in the frequency factor F_B it is preferable for the beam mode-shape factor S_B to equal one so that the actual beam and the beam model can have identical mode shapes. Substitution of Equation (4.8) into Equation (4.4) yields

$$G_I = \frac{G_L^3}{M_{Eb}} \left(\frac{F_B}{S_B} \right)^2 \quad (4.9)$$

Equations (4.8) and (4.9) provide us with the necessary information (G_A and G_I) to scale the beam model down to the appropriate scaling factor G_L . Because the floor is constructed of beams and plates, additional work is needed to scale down the plate, and then to relate the beam and the plate equations.

4.1.1.2 Plate Scaling

The method of scaling down the plate is similar to the method of scaling down the beam. Even though the real plate (a composite of concrete slab and deck) is supported longitudinally by seven parallel joists (see Figure 2.1), the scale model of the plate is assumed to be simply supported on all edges because exact solutions do not exist for the real boundary conditions.

Two significant vibration characteristics that should be considered for the plate model are the natural frequencies and the mode shapes. First, the natural frequencies for the transverse vibration of a scaled-down rectangular plate model, which is made of wood, with a uniform thickness (h) and simply supported edges, can be written as

$$\omega_{scaled}^{rs} = \frac{\pi^2}{4} \left[\left(\frac{r}{a_{sc}} \right)^2 + \left(\frac{s}{b_{sc}} \right)^2 \right] \sqrt{\frac{E_w h_{sc}^2}{\rho_w 12(1 - \nu_w^2)}} \quad r, s = 1, 2, \dots \quad (4.10)$$

where a_{sc} is half the length and b_{sc} is half the width of the plate model. Similar to the beam model's natural frequencies, the frequencies of the scaled-down plate model depend on both the material property of wood (E_w , ρ_w and ν_w) and the scaled-down geometry (a_{sc} , b_{sc} and h_{sc}).

It is convenient to define the following relations for scaling of the plate model's geometry

$$a_{sc}=G_{ab} a_{real} = \text{Half the length of the scaled-down plate model}$$

$$b_{sc}=G_{ab} b_{real} = \text{Half the width of the scaled-down plate model}$$

$$h_{sc}=G_h h_{real} = \text{Thickness of the scaled-down plate model}$$

where G_{ab} is the scaling factor of both the length and the width of the plate and G_h is the thickness-modifying factor.

The following ratios relate the material property of the plate model (E_w , ρ_w and v_w), which is made of wood, to the material property of the real plate (E_{con} , ρ_{con} and v_{con}), which is made of concrete,

$$M_{Ep} = \frac{E_w}{E_{con}} = \text{Modulus of elasticity ratio}$$

$$M_{\rho p} = \frac{\rho_w}{\rho_{con}} = \text{Density ratio}$$

$$M_{vp} = \frac{v_w^2 - 1}{v_{con}^2 - 1} = \text{Poisson first ratio}$$

where E_w is the modulus of elasticity, ρ_w is the density, and v_w is Poisson's ratio of the wood of the plate model. The same material property, but with subscript "con," is related to the actual material of the real plate (concrete). The second subscript p in the material ratios refers to the plate. The plate model's natural frequencies, as given in Equation (4.10), can be expressed now in terms of the real plate's frequencies and the previously defined geometric factors and material ratios

$$\omega_{scaled}^{rs} = \frac{G_h}{G_{ab}^2} \sqrt{\frac{M_{Ep}}{M_{vp} M_{\rho p}}} \frac{\pi^2}{4} \left[\left(\frac{r}{a_{real}} \right)^2 + \left(\frac{s}{b_{real}} \right)^2 \right] \sqrt{\frac{E_{con} h_{real}^2}{\rho_{con} 12(1 - v_{con}^2)}} = F_P \omega_{real}^{rs} \quad (4.11)$$

$$r,s=1,2,\dots$$

where F_P = plate frequency factor

$$= \frac{G_h}{G_{ab}^2} \sqrt{\frac{M_{Ep}}{M_{vp} M_{pp}}} \quad (4.12)$$

Solving Equation (4.12) for G_h yields

$$G_h = F_P G_{ab}^2 \sqrt{\frac{M_{vp} M_{pp}}{M_{Ep}}} \quad (4.13)$$

The thickness-modifying factor G_h depends upon the changes in the material, the geometry, and the frequency. It is preferable that the plate frequency factor F_P equal one so that the actual plate and the plate model can have identical natural frequencies.

A second significant vibration characteristic that should be considered for the plate model is the mode shape. The mode shapes of the scaled-down wooden-plate model can be written as

$$W_{scaled}^{rs} = \frac{1}{\sqrt{\rho_w h_{sc} a_{sc} b_{sc}}} \sin \frac{r\pi}{2a_{sc}} (x_{sc} + a_{sc}) \sin \frac{s\pi}{2b_{sc}} (y_{sc} + b_{sc}) \quad r,s=1,2,\dots \quad (4.14)$$

Similar to the plate model's frequencies, the mode shapes of the scaled-down plate model depend upon the material and the geometry. The scaled-down plate's mode shapes, as given in Equation (4.14), can be expressed now in terms of the real plate's mode shapes and the previously defined geometric factors and material ratios,

$$W_{scaled}^{rs} = \frac{1}{G_{ab} \sqrt{G_h M_{pp}}} \frac{1}{\sqrt{\rho_{con} h_{real} a_{real} b_{real}}} \sin \frac{r\pi}{2a_{real}} (x_{real} + a_{real}) \sin \frac{s\pi}{2b_{real}} (y_{real} + b_{real}) \quad (4.15)$$

$$= S_P W_{real}^{rs} \quad r,s=1,2,\dots$$

where S_P = plate mode-shape factor

$$= \frac{1}{G_{ab} \sqrt{G_h M_{\rho\rho}}} \quad (4.16)$$

Substituting Equation (4.13) into Equation (4.16) yields

$$S_P = \frac{1}{G_{ab}^2} \sqrt{\frac{1}{F_P M_{\rho\rho}}} \sqrt{\frac{M_{Ep}}{M_{vp} M_{\rho\rho}}} \quad (4.17)$$

The plate mode-shape factor S_P depends upon the scaling factor G_{ab} of the plate's length and width, the material ratios, and the square root of the plate frequency factor. It is preferable that the plate mode-shape factor S_P equal one so that the actual plate and the plate model can have identical mode shapes. Equations (4.13) and (4.17) provide us with the necessary information (G_h and S_P) to scale the plate model down to the appropriate scaling factor G_{ab} .

The next important step is to combine the results of the beam- and plate-scaling equations. It is important that both the beam model and the plate model have equal scaling factors ($G_{ab}=G_L$), equal frequency factors ($F_P=F_B$), and equal mode-shape factors ($S_P=S_B$) so that the scaling results for all structural members of the floor scale model will be consistent. If $G_{ab}=G_L$, $F_P=F_B$ and $S_P=S_B$, then we can rewrite the previous Equations (4.8), (4.9), (4.13), and (4.17) in terms of G_{ab} , F_P , and S_P and rearrange them as follows:

$$S_P = \frac{1}{G_{ab}^2} \sqrt{\frac{1}{F_P M_{\rho\rho}}} \sqrt{\frac{M_{Ep}}{M_{vp} M_{\rho\rho}}} \quad (4.18)$$

$$G_h = F_P G_{ab}^2 \sqrt{\frac{M_{vp} M_{\rho\rho}}{M_{Ep}}} \quad (4.19)$$

$$G_A = \frac{1}{G_{ab} M_{\rho b} S_P^2} \quad (4.20)$$

$$G_I = \frac{G_{ab}^3}{M_{Eb}} \left(\frac{F_P}{S_P} \right)^2 \quad (4.21)$$

Because the actual structural material and the scale model material are known, the material ratios (M_E , M_ρ , etc.) for the beams and for the plate can be calculated. The given and the computed material information are shown in Table 4.1.

Table 4.1: The Given and the Computed Material Information

		Girder (Beam)	Joist (Beam)	Concrete Slab (Plate)
Actual Material	Made of	Steel	Steel	Steel & Concrete
	E (psi)	29e6	29e6	2.63e6
	ρ (lb.s ² /in ⁴)	7.3107e-4	0.0012	1.7927e-4
	ν	-	-	0.2
Model Material	Made of	Wood	Wood	Wood
	E (psi)	2.2e6	2.2e6	2.2e6
	ρ (lb.s ² /in ⁴)	8.4e-5	8.4e-5	8.4e-5
	ν	-	-	0.3
Material Ratios (without second subscript)	M_E	0.0759	0.0759	0.8365
	M_ρ	0.1151	0.0679	0.4694
	M_ν	-	-	0.9479

If the scaling factor G_{ab} is 1/6, the frequency factor F_P is one, and the material ratios are given in Table 4.1, then the mode-shape factor S_P and the modifying factors (G_A , G_b , and G_h) are computed by Equations (4.18) through (4.21) and are listed in Table 4.2.

Table 4.2: Initial Scaling Factors

Structural Members	G_{ab}	F_P	S_P	G_A	G_I	G_h
Girder (Beam)	1/6	1	61.5286	0.0138	1.6120e-5	-
Joist (Beam)	1/6	1	61.5286	0.0233	1.6120e-5	-
Plate	1/6	1	61.5286	-	-	0.0203

4.1.1.3 Column Scaling

An adjustment of the stiffness of the four columns is needed until the frequencies of the floor model decrease from 8.4 Hz to 7.3 Hz.

4.1.2 Rescaling the Initial Scale Model of the Floor

In the market, there are only standard dimensions for the beams and the plates that can be used for building the floor model. Thus, rescaling the floor model to the available standard wood dimensions is necessary. The goal of the rescaling process is not to rescale the overall size of the initial scale model of the VPI floor but rather to rescale the initial scaled thickness of the plate model (board). To rescale the thickness, it is necessary to modify the geometric properties of the cross sections of the scaled beams. In other words, while the scaling factor (G_{ab}) and the material (tempered hardboard) of the initial scale model remain the same in the rescaling, there is a change in both the thickness of the scaled plate and the cross-sectional properties of the scaled beams. The focus in the following relations will be on the modifying factors (G_h , G_L , G_A), the frequency factor, and the mode-shape factor. Because the beam and the plate frequency factors are equal $F_P=F_B$, it can be determined from the beam and the plate frequency factor Equations (4.3) and (4.12) that

$$\frac{G_I}{G_A} = G_h^2 \quad (4.22)$$

Also, because the beam and the plate mode-shape factors are equal $S_P=S_B$, it can be determined from the beam and the plate mode-shape factor Equations (4.6) and (4.15) that

$$G_h=G_A \quad (4.23)$$

Introducing Equation (4.23) into Equation (4.22) and multiplying both sides by G_A yields

$$G_I=G_A^3 \quad (4.24)$$

As a result, the frequency factor for both the beam and the plate is

$$F_P=G_h \quad (4.25)$$

and the mode-shape factor for the beam and the plate is

$$S_P=\frac{1}{\sqrt{G_h}} \quad (4.26)$$

The rescaling process depends upon the rescaled thickness-modifying factor (G_{rh}). This factor is the ratio of the required thickness of the plate model to the initial scaled thickness of the plate model. If the required plate thickness in the model is h_{req} , then the rescaling equations, given by Equation (4.22) through (4.26), can be summarized and rewritten with the first subscript notation r in terms of h_{req} , h_{sc} and G_{rh} as follows:

$$G_{rh} = \frac{h_{req}}{h_{sc}} \quad (4.27)$$

$$G_{rA} = G_{rh} \quad (4.28)$$

$$G_{rI} = G_{rh}^3 \quad (4.29)$$

$$F_{rP} = G_{rh} \quad (4.30)$$

$$S_{rP} = \frac{1}{\sqrt{G_{rh}}} \quad (4.31)$$

These rescaling equations do not include the effect of scaling, as given in Equations (4.18) through (4.21). If $h_{real}=3$ in. and $G_h=0.0203$, then $h_{sc}=.0609$ in. With $h_{req}=1/8$ in., Equations (4.27) through (4.31) can be used to find the rescaling factors. These factors are listed in Table 4.3.

Table 4.3: Rescaling Factors

Structural Members	F_{rP}	S_{rP}	G_{rA}	G_{rI}	G_{rh}
Girders	2.0567	0.6973	2.0567	8.7000	-
Joists	2.0567	0.6973	2.0567	8.7000	-
Plate	2.0567	0.6973	-	-	2.0567

4.1.3 The Final Scale Model of the Floor

Combining the results of scaling for the beam and the plate models, as given previously in Equations (4.18) through (4.21), and the results of rescaling, as given in Equations (4.27) through (4.31), gives the following final scaling equations, which are denoted with the first subscript F :

$$G_{Fh} = G_{rh} G_h \quad (4.32)$$

$$G_{FA} = G_{rA} G_A \quad (4.33)$$

$$G_{FI} = G_{rI} G_I \quad (4.34)$$

$$F_{FP} = F_{rP} F_P \quad (4.35)$$

$$S_{FP} = S_{rP} S_P \quad (4.36)$$

Providing the initial scaling factors in Table 4.2 and the rescaling factors in Table 4.3, Equations (4.32) through (4.36) give the final scaling factors, listed in Table 4.4. Due to the significance of the scaling factor (G_{ab}), it is also included in Table 4.4.

Table 4.4: Final Scaling Factors

Structural Members	G_{ab}	F_{FP}	S_{FP}	G_{FA}	G_{FI}	G_{Fh}
Girders	1/6	2.0567	42.9033	0.0283	1.4024e-4	-
Joists	1/6	2.0567	42.9033	0.0480	1.4024e-4	-
Plate	1/6	2.0567	42.9033	-	-	0.0417

At this point, all of the dimensions of the scaled plate (board) can be computed easily. The concrete slab with the metal deck of the real VPI floor has a length of 300 in., a width of 180 in., and a thickness of 3 in. Because the actual dimensions of the concrete slab are known, the final scaling factors (G_{ab} , G_{Fh}) in Table 4.4 help to compute the final dimensions of the board. As a result, this board is 50 in. long, 30 in. wide, and 1/8 in. thick.

On the other hand, the cross-sectional dimensions of the scaled beams still need more analytical work in order to be specified. The wooden beams in the scale model are selected to have rectangular cross sections with width w_{sc} and height t_{sc} . Therefore, the following relations for the area moment of inertia and the cross-section area are helpful:

$$I_{sc} = \frac{w_{sc} t_{sc}^3}{12} \quad (4.37)$$

$$A_{sc} = w_{sc} t_{sc} \quad (4.38)$$

Solving Equations (4.37) and (4.38) for the unknown width w_{sc} and height t_{sc} of the scaled beam yields

$$w_{sc} = \sqrt{\frac{A_{sc}^3}{12 I_{sc}}} = \sqrt{\frac{G_{FA}^3 A_{real}^3}{12 G_{FI} I_{real}}} \quad (4.39)$$

$$t_{sc} = \sqrt{\frac{12 I_{sc}}{A_{sc}}} = \sqrt{\frac{12 G_{FI} I_{real}}{G_{FA} A_{real}}} \quad (4.40)$$

Table 4.5: Geometric Properties of the Real Beams

Geometric Properties	Girders	Exterior Joists	Interior Joists
Beam Length (in)	180	300	300
Cross-Sectional Area (in ²)	6.49	1.9	1.9
Area Moment of Inertia (in ⁴)	199	166	171.8

Because the final scaling factors (Table 4.4), and the geometric properties of the real girders and joists (Table 4.5) are known, the width w_{sc} and height t_{sc} of the scaled girders and joists can be calculated by Equations (4.39) and (4.40). The given information is shown in Table 4.4 and Table 4.5, and the results are listed in Table 4.6. G_{ab} is important to compute the new length of the beams. The final dimensions for the scaled beams of the VPI floor scale model are given in Table 4.6. Figure 4.1 shows the wooden frame of the scale model of the VPI floor.

Table 4.6: Geometric Properties of the Scaled Beams

Geometric Properties	Girders	Exterior Joists	Interior Joists
Beam Length (in)	30	50	50
Cross-Sectional Width (in)	0.1362	0.0521	0.0512
Cross-Sectional Height (in)	1.3499	1.7500	1.7803
Cross-Sectional Area (in ²)	0.1838	0.0912	0.0912
Area Moment of Inertia (in ⁴)	0.0279	0.0233	0.0241

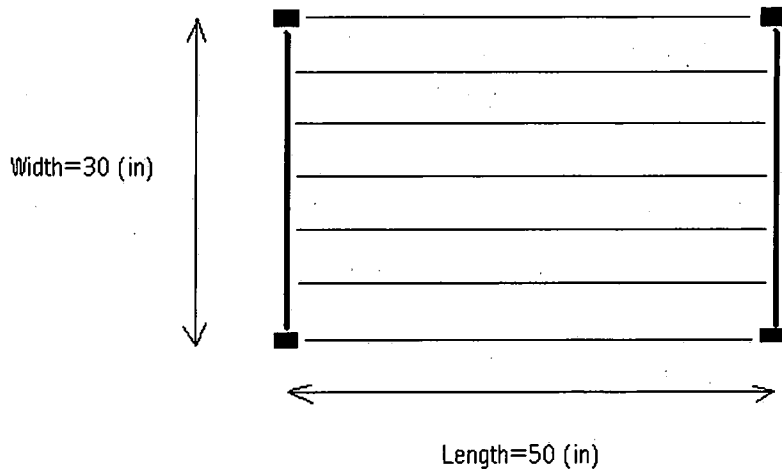


Figure 4.1: Top View of the Wooden Frame of the Final Floor Scale Model

4.1.3.1 The Actual Floor Frequencies

Consider the effect of adding mass to the floor model on the floor resonant frequency. Fortunately for both the beam and the plate, there is a relation between the natural frequencies and the mass. The natural frequencies of the beam model and the plate model are inversely proportional to the square root of their masses (see Equations (4.1) and (4.10)). That is, the frequency decreases as the mass increases.

$$\omega \propto \frac{1}{\sqrt{m}}$$

Even though this shows the relation between the natural frequency of the structural member and its own mass, this relation seems to be valid between the natural frequency and the mass that rests on the structural member. Therefore, several masses are placed on top of the floor model so that the frequencies of all of the structural members, and eventually the entire floor, decrease. The combined mass of the floor mass m and the added masses, whose total mass is three times the mass of the floor ($m_{added}=3m$), is

$$m_{comb} = m + m_{added} = m + 3 m = 4 m$$

The frequency for the floor model with the added mass ω is half of the frequency for the floor model without the added mass ω_{scaled} :

$$\omega = \frac{1}{\sqrt{4}} \omega_{scaled} = \frac{1}{2} \omega_{scaled} = \frac{1}{2} (F_{FP} \omega_{real}) = \frac{1}{2} (2.0567 \omega_{real}) \approx \omega_{real}$$

Similarly, the mode shapes for the scale model with the added mass W is half of the mode shape for the scale model without the added mass W_{scaled} :

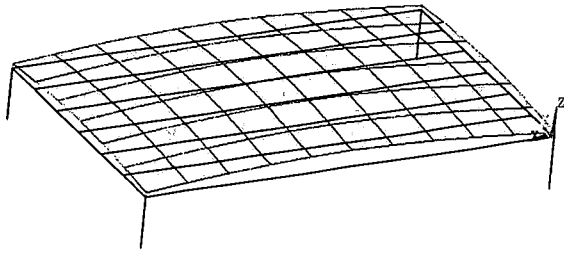
$$W = \frac{1}{\sqrt{4}} W_{scaled} = \frac{1}{2} W_{scaled} = \frac{1}{2} (S_{FP} W_{real}) = \frac{1}{2} (42.90 W_{real}) \approx 21 W_{real}$$

As a result, the natural frequencies of the scale model of the floor with the added mass are almost the same as the natural frequencies of the actual floor. However, the mode shapes of the floor model with the added mass are about twenty-one times the mode shapes of the actual floor. This indicates that the vibration amplitudes of the floor scale model are much larger than the amplitudes of the actual floor.

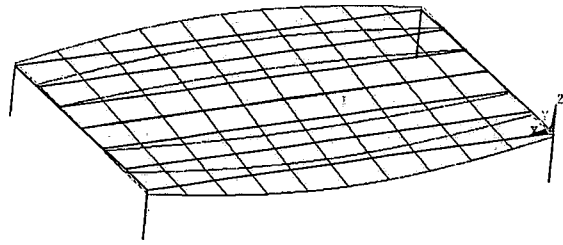
To verify the accuracy of the proposed scaling procedure analytically, the scale model of the VPI floor is modeled in ANSYS. Similar to the VPI floor in Chapter 2, shell elements (Shell 63) are used for the concrete slab, and beam elements (Beam 4) are used for the girders and the joists. The material properties for the tempered hardboard in Table 4.1 and the geometric properties for both the board (50 in. by 30 in. by 1/8 in.) and the scaled beams in Table 4.6 are used for constructing the finite-element model of the floor scale model. Similar to the VPI floor in Chapter 2, the four columns are modeled as springs (Combination 14). Here, the stiffness of the four springs needs to be adjusted equally so that the first natural frequency of the floor model decreases from about 8.1 Hz

to 7 Hz. In this finite-element model, a uniform distributed mass accounting for the live masses is applied on the floor model.

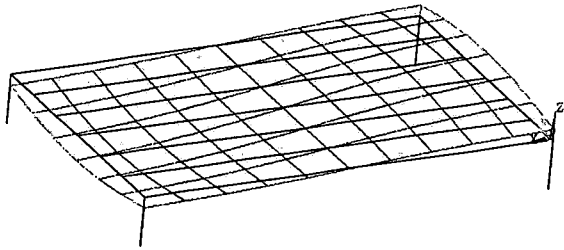
Even though this structure is sophisticated, the finite-element results show that the developed scaling procedure leads to a very accurate scale model with the expected scaling results. Figure 4.2 shows the mode shapes of the first five modes of the floor scale model. The natural frequencies of the VPI floor scale model are approximately equal to the frequencies of the full-scale VPI floor (Chapter 2). The pattern of the finite-element deformed shape at every natural frequency of the floor scale model (Figure 4.2) and the full-scale floor model (Figure 2.2) are identical. For example, the first mode shape at 7 Hz has the expected half-sine shape on all sides of the floor. While the natural frequencies and the mode shapes are considered in both the scaling procedure and the finite-element modeling, the modal damping ratios are not considered and cannot be predicted precisely. The finite-element results of the wooden scale model of the VPI floor are very encouraging.



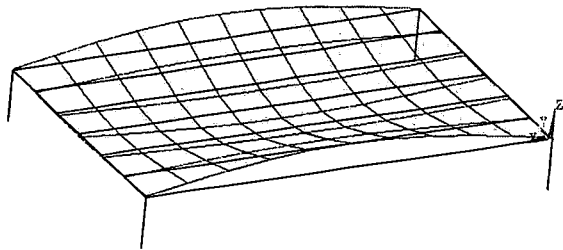
First Mode Shape at $f_1=7.00$ Hz



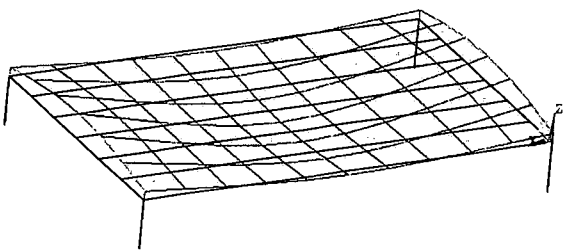
Second Mode Shape at $f_2=10.34$ Hz



Third Mode Shape at $f_3=15.99$ Hz



Fourth Mode Shape at $f_4=16.98$ Hz



Fifth Mode Shape at $f_5=27.73$ Hz

Figure 4.2: The First Five Mode Shapes of the Floor Finite-Element Scale Model with the Added Mass

After choosing the sizes and the materials of the structural members in the design phase, the next major task is the construction of the floor scale model. Depending upon the previously described geometric and material properties of the structural members, the wooden scale model of the VPI floor is built. Not only is the floor made of wood, but the four columns are wooden, as well. Each wooden column has a length of 27 in. and has a rectangular cross section with a width of 1.5 in. and a height of $\frac{1}{2}$ in. Six small, uniform

bricks are distributed evenly on the floor. Figure 4.3 shows a photograph of the VPI floor scale model with the added masses.

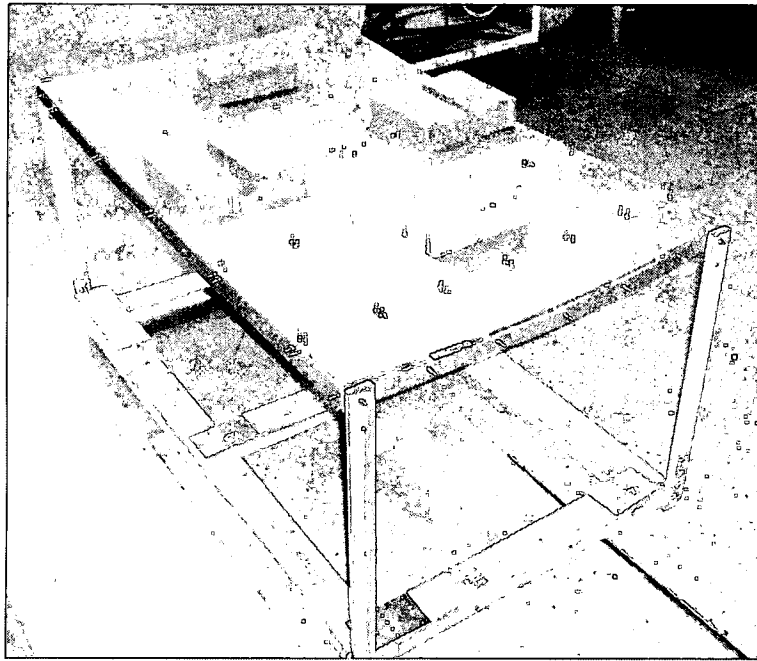


Figure 4.3: The Wooden Scale Model of the VPI Floor with the Added Masses

To extract the modal parameters of the floor scale model, experimental tests are conducted in order to obtain the frequency response of the floor. The first mode is of a great concern in this study. Because its antinode is located at the center of the floor, measurements of the frequency response are recorded there. The experimental frequency response is shown in Figure 4.4. Within the measured frequency range of 4 Hz to 16.5 Hz, there are two dominant vibration modes, which are indicated by the two peaks (see Figure 4.4). These two modes represent the first and third modes of vibration. For the first four modes of vibration, the measured natural frequencies of the VPI floor scale model are approximately the same as the natural frequencies of the full-scale VPI floor. For example, the first natural frequency of the VPI floor scale model is about 7 Hz, similar to the full-scale VPI floor.

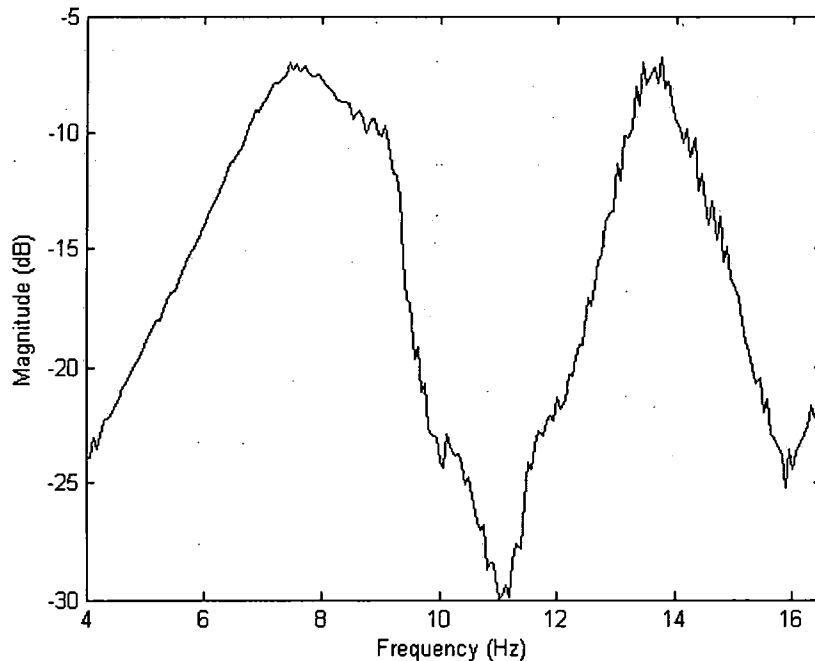


Figure 4.4: The Experimental Frequency Response of the Floor Scale Model

Unfortunately, this scale model of the VPI floor has an adequate amount of inherent damping. The equivalent viscous damping ratio of the first mode is about 13.5%. This damping ratio is computed by means of the half-power method, which will be described in greater detail in Chapter 5. This large amount of damping is due to both the material and the joint connections of the floor model. Frequently, nonmetallic materials, such as tempered hardboard, have much more damping than metallic materials. In addition, the structural members of this floor model are bolted together. The dry friction between the surfaces at the bolted joints produces additional damping to the system [11]. It is obvious that this floor scale model cannot be used to verify the effectiveness of the 3-DOF TMD because of its large amount of damping.

4.2 The Steel Scale Model of the VPI Floor

Therefore, another scale model of the VPI floor was considered. A great effort was made to choose the appropriate material and proper connections at the joints of the new floor model so that it will have the minimum amount of damping. Accordingly, the best option available was metal because it typically produces a low amount of damping. For this model, we chose steel, which has a modulus of elasticity of 29×10^6 psi, a mass density of 7.34599×10^{-4} lb.s²/in.⁴, and a Poisson ratio of 0.32. Rao [11] suggested considering the welded joints instead of bolted joints to minimize the internal damping in the connections. Therefore, the structural members are welded together.

The procedure for scaling the new floor scale model is similar to the procedure for scaling the wooden floor model. In this new floor model, the scaling factor is the same as in the wooden floor model: $G_{ab}=1/6$. The MATLAB m-file, which was developed earlier for computing the parameters of the wooden scale model, is utilized here to calculate the parameters of the steel scale model of the VPI floor. This initial scaling procedure produces a thickness of 0.049 in. for the scaled plate model. Because the minimum available thickness for the plate is 0.0897 in., it is necessary to rescale the whole scale model to meet the required (or available) thickness dimension. The beams of the steel scale model, like those of the wooden scale model, have rectangular cross sections.

The MATLAB m-file provides the final scaling factors and the final dimensions of the structural members of the steel scale model. The final scaling factors are listed in Table 4.7. The 0.0897-in.-thick steel plate has a length of 50 in. and a width of 30 in. The final dimensions for the scaled beams of the steel floor model are listed in Table 4.8. Because the scaling factor $1/6$ is used for scaling both the wooden floor model and the

steel floor model, the floor plan in Figure 4.1 is valid for both floor models. The picture in Figure 4.5 shows the steel scale model of the VPI floor.

Table 4.7: Final Scaling Factors

Structural Members	G_{ab}	F_{FP}	S_{FP}	G_{FA}	G_{FI}	G_{Fh}
Girders	1/6	1.83	17.14	0.0203	0.5254e-4	-
Joists	1/6	1.83	17.14	0.0345	0.5254e-4	-
Plate	1/6	1.83	17.14	-	-	0.0299

Table 4.8: The Final Dimensions of the Scaled Beams

Geometric Properties	Girders	Exterior Joists	Interior Joists
Beam Length (in)	30	50	50
Cross-Sectional Width (in)	.1352	.517734e-1	.508919e-1
Cross-Sectional Height (in)	.975339	1.26442	1.28632

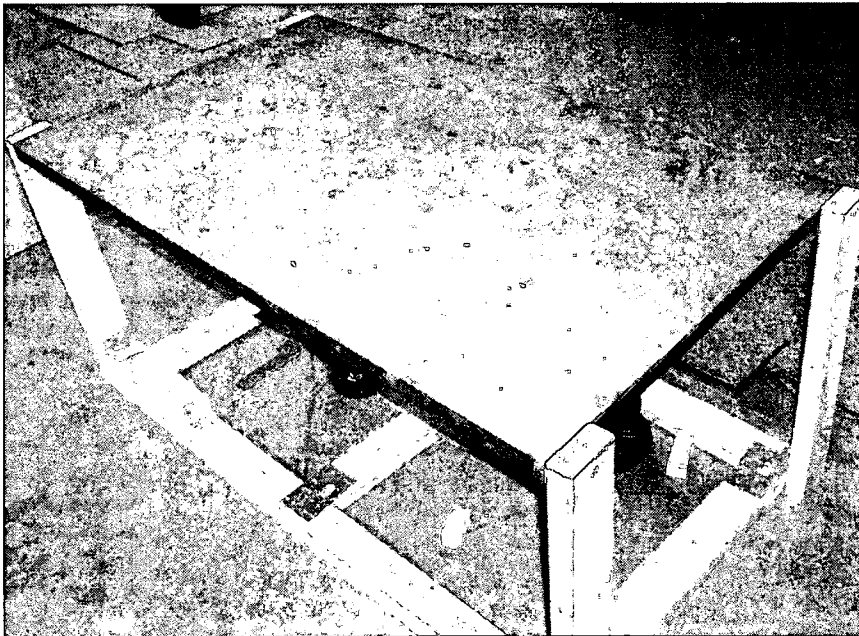


Figure 4.5: The Steel Scale Model of the VPI Floor

As shown in Table 4.7, the natural frequencies of the scale model are about 1.83 times larger than the natural frequencies of the real VPI floor (i.e., $F_{FP}=1.83$). Also, the mode-shape factor S_{FP} is 17.14. The measured natural frequencies of the steel floor model are increased by a factor of 2.5. The increase in the natural frequencies from the frequency factor of 1.83 to a factor of 2.5 stems from the following causes:

1. Inaccurate dimensions for the structural members of the steel floor model
2. A difficulty in decreasing the stiffness of the four columns (smaller cross-section area) for safety reasons
3. The difference between the types of connections that are used in the real VPI floor and the connections that are used in the steel floor model

Similar to the wooden floor model, concentrated masses are distributed throughout the top surface of the steel floor model in order to make the vibration characteristics more similar to the real VPI floor. These masses on the steel floor model have a strong effect on the model's modal properties (natural frequencies, mode shapes, damping ratio). The total weight of these masses is about 222 lbs. Increasing the masses on the floor model results in a decrease in its natural frequencies. The 222-lb. total weight decreases the natural frequencies to about half of the original values. For example, the first significant natural frequency decreases from 18 Hz to about 9 Hz.

With these masses on the floor model, the damping ratio of the first mode also decreases from about 9% to 5.8%. One major difference between the steel scale model of the VPI floor and the wooden scale model is that the first has much less damping than the second. Due to these vibration characteristics, especially the first mode's low damping, the steel scale model of the VPI floor is selected to be used for verifying the effectiveness

of the 3-DOF TMD. Additional information about the vibration characteristics of the steel scale model will be presented in the next chapter.

CHAPTER V

EXPERIMENTAL RESULTS

To determine experimentally the modal parameters--i.e., the natural frequencies, mode shapes, and damping ratios--the frequency response function (FRF) of a vibrating system needs to be measured and analyzed. For the experimental work that is involved in this dynamic analysis, the FRF is extremely useful for determining the natural frequencies and damping ratios. Knowing these important vibration parameters can help to understand the dynamic system, improve its dynamic behavior and modify its design if needed [11].

One of the most important reasons for performing the experimental tests in this study is to evaluate the damping presented in the test system with and without damping treatments. Among the system parameters (mass, stiffness, damping), the damping is not easy to quantify accurately [26]. The deficiency of the analytical damping models is due to the type of the required test [29]. Static tests can be used in order to determine accurately the mass and stiffness of a system, but dynamic tests are necessary for determining the amount of damping [26]. Damping is not easy to model and predict mathematically [17]. However, the amount of damping present in a system can be

measured easily. The damping ratio can be determined experimentally by analyzing the FRF of the oscillating system.

By examining the experimental frequency response of the system, the modal parameters can be extracted easily. Each mode of vibration of the test system is indicated by a distinct peak in the frequency response magnitude. The location of each resonant peak on the frequency axis identifies the natural frequency of the mode [26]. The sharpness or height of the resonant peak in the frequency response indicates the amount of damping present in the mode of vibration [28]. By using the half-power method, the bandwidth reveals quantitatively the amount of damping in that mode. The bandwidth measures the width of the resonant peak and represents the frequency range between the two frequencies ω_a and ω_b , which are on either side of the resonant frequency ω . These two frequencies correspond to the half-power points, which are lower in magnitude (dB) than the resonant peak by 3 dB. The damping ratio can be found as $\zeta = \frac{\omega_b - \omega_a}{2\omega}$.

The equipment that is needed and has been used for performing the vibration experiments of this study are the shaker, accelerometer, dynamic signal analyzer, and power amplifier. The shaker excites the test system (floor, beam system) according to the predefined function set earlier on the analyzer, the accelerometer measures its response, the analyzer evaluates this response, and the power amplifier modifies the actuation signal that is sent from the analyzer to the shaker. These hardware components and the included multifunction software in the analyzer provide enough experimental means for doing several types of vibration tests and measurements. In order to extract the modal parameters, it is important to measure the frequency response of the test structure.

5.1 Absorbers

The goal of this chapter is to verify the effectiveness of the 3-DOF TMD experimentally. In Chapter 3, the ability of the 3-DOF TMD in reducing the vibration of the full-scale model of the VPI floor was shown analytically. This chapter is the experimental extension of the analytical work discussed in Chapter 3. Here, a prototype of the 3-DOF TMD is designed to be tested on the steel scale model of the VPI floor, which was described in detail in Chapter 4. Before evaluating the entire system of the 3-DOF TMD, it is necessary to focus on the basic unit of the 3-DOF TMD: the absorber. Even though different aspects of the absorber design will be evaluated, the main focus will be on damping.

For best performance of the 3-DOF TMD, each of the three absorbers should have damping in the range of 3% to 7%. Every absorber consists of a cantilevered beam and a mass at the tip. An absorber with a beam that is made and constructed from one solid cross section (one layer) of metal (steel or aluminum) has very low damping. It is important to determine the exact amount of damping in the absorber. Depending upon the amount of damping present, more damping may need to be introduced to the absorber in order to meet the required damping of the absorber ($3 \leq \zeta \leq 7$). The purpose of the following experiments is to evaluate the damping presented in the absorber with and without damping treatments.

First, consider the absorber without damping treatment. As previously mentioned, the absorber is composed of a cantilevered beam and a concentrated mass at its tip. Here, the uniform beam is constructed from one strip (layer) of aluminum. The beam has a length of 5.25 in. and has a rectangular cross section with a width of 1 in. and a height of

1/8 in. A concentrated mass of 6.55×10^{-3} lb.s²/in. (a weight of approximately 2.5 lbs.) is bolted to the tip of the beam. At this point, all of the important properties of the absorber components (i.e., beam, mass) are defined.

It is important to connect the sensor and the shaker to the beam-mass system at the appropriate locations. The root of the beam is fixed to the shaker, and the motion sensor is connected to the tip of the beam. A harmonic force with a frequency range of 4 Hz to 16.5 Hz is applied at the root of the beam by the shaker. The measured magnitude of the frequency response at the tip of the beam is shown in the (top) dashed line in Figure 5.1.

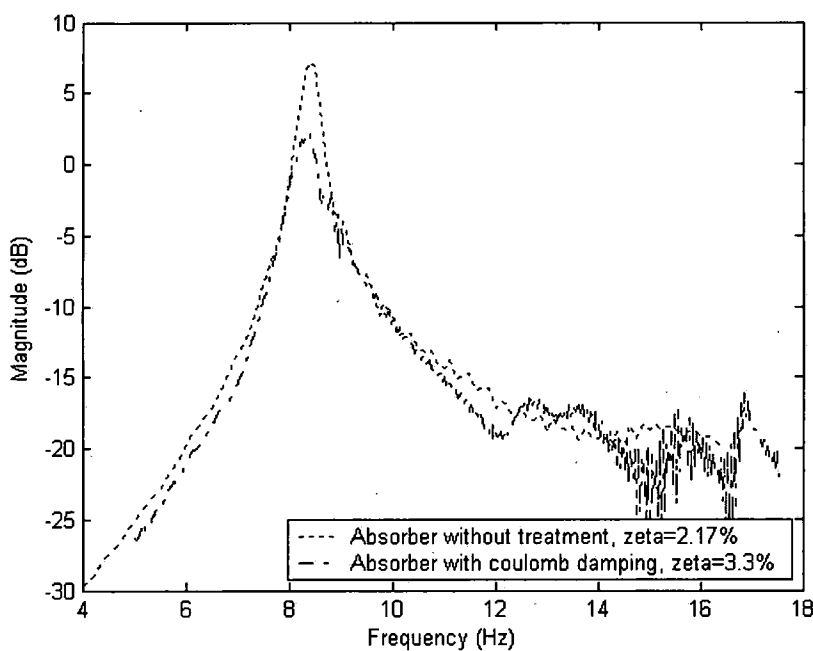


Figure 5.1: Absorber Without and With Coulomb Damping

The experimental frequency response helps to identify the modal parameters in the frequency range of 4 Hz to 16.5 Hz. Within this range, there exists only one resonant peak and, as a result, the system has only one mode. The end mass vibrates at the frequency of 8.37 Hz. By using the half-power method, the modal damping ratio of the

vibrating beam is 2.17%. This amount of damping represents only two-thirds of the minimum required damping for each absorber. Therefore, additional damping should be introduced to the absorber by a proper way.

It is important to provide the necessary damping to the absorber artificially. The damping can be introduced into the beam system in two different approaches: coulomb damping and the use of viscoelastic damping material. In both approaches, there is a special design for the cantilevered beam with an end mass.

The first approach to add more damping to the absorber is coulomb damping. In this approach the cantilevered beam is constructed from two identical aluminum strips that are bolted together along their length. Each strip is rectangular in cross section with a width of 1 in. and a height of 1/16 in. The length of every strip is 5.25 in. The two joining bolts are spaced equally and are very small. Similar to the absorber without damping treatment, a mass of $6.55 \times 10^{-3} \text{ lb.s}^2/\text{in.}$ is attached to the tip of the two-layer beam. The fasteners (bolts) are tight so that the two strips come in contact along their length. When the beam vibrates, the strips are deflected repeatedly and slide relative to each other. Because the two aluminum strips have smooth surfaces, they produce little friction when they are rubbed against each other. Therefore, the contacting surfaces are rubbed down with sandpaper in order to create rough surfaces. When the two strips with treated surfaces are rubbed together rapidly while they are vibrating, the friction produces more damping. With coulomb damping, the damping ratio of the absorber increases from 2.17% to 3.3%, into the appropriate damping range. The center-line trace in Figure 5.1 depicts the FRF of the absorber with coulomb damping.

The other major approach for providing more damping to the absorber is to add viscoelastic material. An effective way to use this approach is to design the beam specifically with an extra-thin layer of viscoelastic material sandwiched between the two aluminum strips. Here, the dimensions and the material of the strips are identical to the ones in the absorber with coulomb damping. Similarly, the end mass is the same one in the previous approach. Because of the high amount of shear deformation in the middle viscoelastic layer, the new sandwich-beam system has a significant amount of damping. The damping of the absorber with viscoelastic material increased from 2.17% to 9.94%. This damping material not only increases the amount of damping present in the new system, but also increases its stiffness slightly.

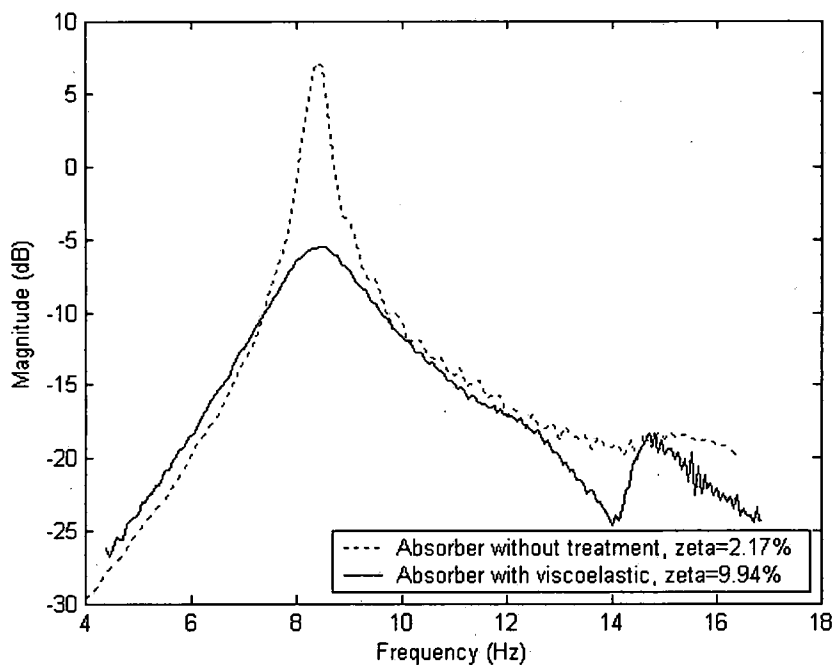


Figure 5.2: Absorber Without and With Viscoelastic Material

The amount of damping increases as the viscoelastic damping material increases. The presence of viscoelastic damping material along the beam length (the whole seam)

results in an increase in the amount of damping up to 10%. To introduce reasonable damping to the absorber ($3 \leq \zeta \leq 7$), the viscoelastic material needs to be added to only a portion of the seam.

In both damping treatments, two identical aluminum strips are joined to provide additional damping to the absorber. In both damping-treatment approaches, the sum of the cross-sectional heights of the two identical strips is equal to the height of the beam without damping treatment. The width of either strip in both damping approaches is equal to the width of the beam without damping treatment.

However, there are some differences between the two major types of damping. One main difference between the coulomb damping and the viscoelastic material is that the latter provides much more damping. Also, they differ in that the viscoelastic damping gives a smooth frequency response while the coulomb damping gives a noisy frequency response. The rough response of coulomb damping is due to the presence of nonlinear, dry friction in the process.

5.2 The 3-DOF TMD

After the absorber with viscoelastic material reveals reasonable damping by showing one peak with a reasonable height in the FRF, it is important to verify the effectiveness of the 3-DOF TMD. Thus far, these ideas regarding the 3-DOF TMD are only theoretical and have not been tested experimentally. Therefore, a prototype of the 3-DOF TMD is developed and used experimentally in the floor scale model to demonstrate the design, tuning, and effectiveness.

Choosing the proper locations for exciting the floor model and measuring its response is quite important. Because the first mode of vibration has its antinode at the center of the floor, both the accelerometer and the shaker are placed near the center of the floor model. The accelerometer is located on the floor model and the shaker is located under the floor model. The shaker, which stands in an upright position, is connected to the floor by a stinger. Here, the stinger is a slender, threaded nylon rod with a length of about 3.5 in. This vertical member is positioned at right angles to the floor.

In order to determine the modal parameters of the floor model, the frequency response of this structure was measured experimentally. The magnitude of the frequency response, which is shown in Figure 5.3, exhibits three sharp, distinct peaks. These three peaks indicate that this simple laboratory model has three modes of vibration within the measured frequency range of 4 Hz to 16.5 Hz. These three modes (or peaks) are well-spaced (spaced by at least 2 Hz) and located at frequencies of 7 Hz, 9.375 Hz, and 13.1 Hz.

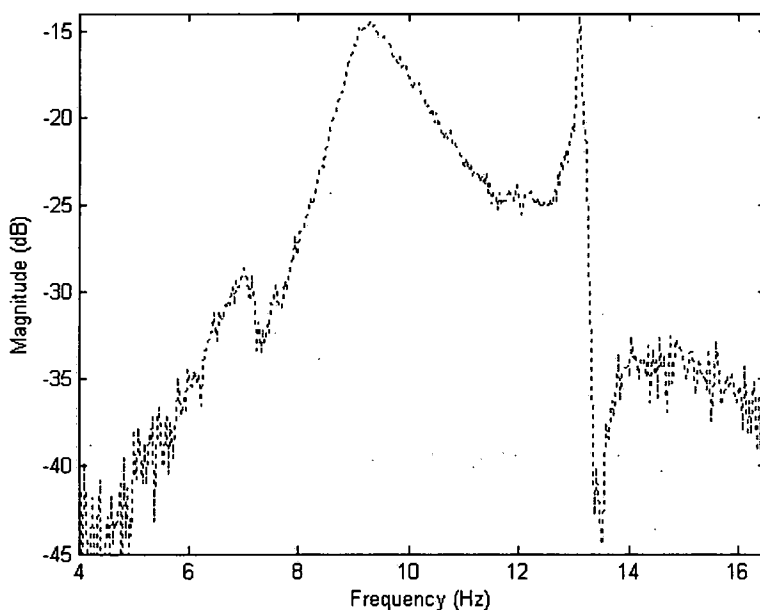


Figure 5.3: Frequency Response of the Floor Scale Model

The first vibration mode at about 7 Hz. arises due to the scaling process of the full-scale floor to the scale model of the floor. Because this mode is much smaller in magnitude than the other two modes (i.e., it is hard to observe in the FRF) and does not exist in the real floor, it will be neglected in this experimental work. Therefore, in the remaining part of this study the first two significant modes at 9.375 Hz and 13.1 Hz. are referred to as the first mode and second mode of vibration, respectively.

The second mode of vibration, at 13.1 Hz, has a longitudinal nodal line that passes through the center of the floor. Due to this fact, the second mode should not be observed in the frequency response at the center of the floor. However, the accelerometer is a few inches away from the center of the floor, not exactly at the center. As a consequence, the peak of the second mode at the frequency 13.1 Hz appears in the experimental response.

The first two modes make meaningful contributions to the bending vibration of the floor scale model. The natural frequencies and the computed modal damping ratios of the first two modes are provided in Table 5.1.

Table 5.1: Experimental Floor Modal Parameters

Mode	Frequency (Hz)	Damping (%)
1	9.375	5.8
2	13.1	1

Between the first two modes of vibration, the first mode (i.e., fundamental mode) is more critical to the floor response (more energy). The fundamental mode has a natural frequency of 9.375 Hz, a maximum amplitude (antinode) at the center of the floor, and a

damping ratio of 5.8%. This mode, which is denoted by the first sharp peak in Figure 5.3, is well-spaced from the second mode and has low damping.

Because the typical TMD is more effective with a structure that has very low damping ($\zeta < 3\%$) and the proposed 3-DOF TMD has the same ability of the typical TMD, the effectiveness of the 3-DOF TMD to control the first mode of the floor model is limited due to the first mode's relatively high damping ($\zeta = 5.8\%$). Without any treatment, the transient response of this floor model, which has high damping, needs only a few cycles to die out or to have negligible amplitude. Clearly, this floor model does not necessarily need a TMD for the first mode because it already has reasonable damping.

Similar to the analytical study, a single 3-DOF TMD is placed at the center of the floor to control the fundamental mode, which has its antinode also at the center of the floor. The goal of using the 3-DOF TMD is not to show its full effectiveness because of the reasons mentioned earlier, but rather to illustrate the design and the tuning process, as well as to show some of its effectiveness. Therefore, a prototype of the proposed 3-DOF TMD is designed to be placed and tested at the center of the steel scale model of the VPI floor. Fortunately, this particular location is the best position for the 3-DOF TMD because it allows the TMD to expand on a horizontal plane that is parallel to the floor plane.

For the 3-DOF TMD, there are three design variables: mass ratio μ , optimal tuning frequency ratio f_{opt} , and the damping ratio ζ . The mass ratio is chosen to be 5.5% for the 3-DOF TMD. Because this TMD has three absorbers, each of the absorbers has only one-third of this ratio. As a result, the mass ratio of each absorber is 1.83%. The second design variable, the optimal-tuning frequency ratio f_{opti} , is determined for each

absorber by means of analytical simulations in MATLAB. This ratio allows us to obtain the optimal frequency of the absorber theoretically.

A few preliminary experiments are conducted in this study to evaluate the necessary damping for each absorber. The experimental results show that the minimum amount of damping necessary for each absorber is about 6%. This is twice the damping that was selected for the analytical model of the absorber in Chapter 3. This difference in the amount of damping between the analytical models in Chapter 3 and the laboratory models in this chapter is due to many reasons. First, the analytical full-scale floor model has a damping ratio of only 0.5%, but the laboratory floor model has a much higher damping ratio of 5.8%. Second, unlike the analytical model of the 3-DOF TMD, which has a mass ratio of 5%, the prototype of this TMD has a mass ratio of 5.5%. Thus, a damping ratio of 6.8% is considered for each absorber of the 3-DOF TMD.

Since the first mode contains a great percentage of the floor energy and the 3-DOF TMD is tuned to this mode, the floor model can be modeled roughly with the first mode of vibration. The floor-model parameters are determined by the modal parameters that are obtained by the finite-element package ANSYS.

Depending upon the floor-model parameters and design variables, the simulation and tuning process (described completely in Chapter 3) are carried out numerically in MATLAB. This analytical simulation is helpful not only to determine the optimal values of the three absorber frequencies, but also to identify the two new resonant peaks. Following the step-by-step procedure for tuning the three absorbers provides a theoretical starting point. Analytically, the frequency-response function of the floor model with and

without the 3-DOF TMD is shown in Figure 5.4. The optimal values of the three absorbers' parameters are listed in Table 5.2.

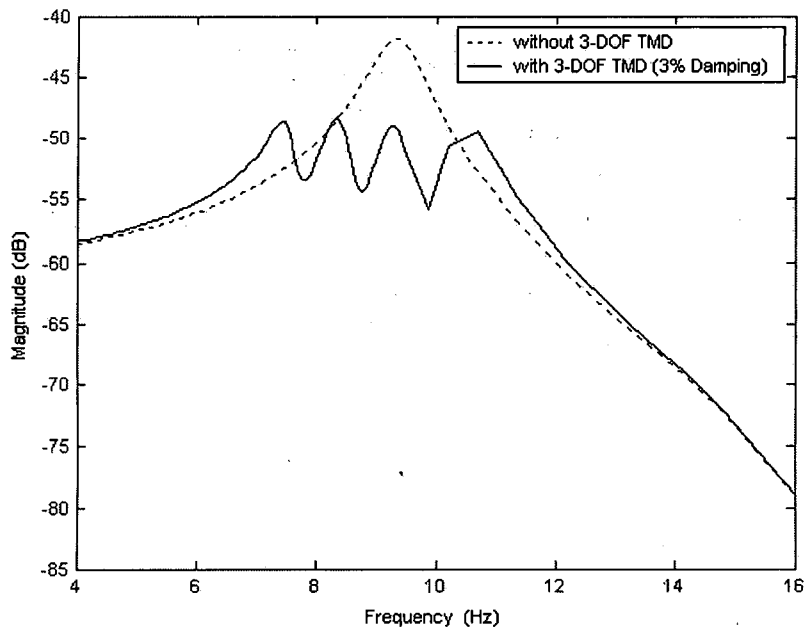


Figure 5.4: Frequency Response Magnitude of the Floor Model With and Without the 3-DOF TMD

Table 5.2: 3-DOF TMD Absorbers' Parameters

Absorber Parameters		VA1	VA2	VA3
f_n	Hz	9.38	8.38	9.71
f_{opti}	-	.93	.922	1.01
f_t	Hz	8.72	7.73	9.81
μ	%	1.83	1.83	1.83
ζ	%	3	3	3
m_t	lb.s ² /in	6.55e-3	6.55e-3	6.55e-3
k_t	lb/in	19.66	15.44	24.88
c_t	lb.s/in	21.53e-3	19.09e-3	24.23e-3

The MATLAB simulation shows a very important fact in Figure 5.4. The four new resonant peaks in magnitude are lower than the original peak by only about 7.5 dB.

However, the analytical simulation in Chapter 3 shows a much more significant reduction in the magnitude for the full-scale model of the VPI floor with the 3-DOF TMD. Figure 3.4 shows that the four new resonant peaks in magnitude are lower than the original peak by about 23 dB. This big difference in the reduction of the magnitude between the floor model with the 3-DOF TMD in Chapter 3 and the floor scale model with the 3-DOF TMD in this chapter is due to the amount of damping presented in the floor systems. The full-scale model of the VPI floor has a damping of 0.5%, but the scale model of the floor has a damping of 5.8%.

As discussed in Chapter 3, the 3-DOF TMD consists of three absorbers. Each absorber is composed of a cantilevered beam and a concentrated mass attached at its tip. The absorber in the form of a beam with an end mass functions as a spring-mass system. Here, the beam represents the spring, and the end mass represents the mass of the spring-mass system.

After deciding on the configuration of the 3-DOF TMD, the next design step is to choose the material and the cross-sectional dimensions of the three beams. For the beams of the 3-DOF TMD, we need a material that is elastic. Even though steel is typically the primary choice, aluminum has some important advantages over steel for this study. Aluminum is easy to cut, available in the market with a very thin height, and lighter in weight. Thus, aluminum is the best choice for the three beams in this model. The modulus of elasticity of this material is 8×10^6 psi. Each beam has a rectangular cross-section with a width of 1 in. and a height of 1/8 in. This represents the overall cross-sectional dimensions without the viscoelastic material.

The final step of the initial design of the 3-DOF TMD is to determine both the masses at the tips of the beams and the lengths of the three beams. The beams are made of aluminum, their cross-sectional shapes are defined (i.e., $b = 1$ in. and $h = 1/8$ in.), and the simulation parameters are provided in Table 5.2. As a result, the end masses and the lengths of the three beams can be computed using the equivalent mass and stiffness relations (i.e., $M=m_t$ and $L = (3 E I / k_t)^{1/3}$). These results are listed in Table 5.3.

Table 5.3: Initial Design Parameters of the 3-DOF TMD

Absorber Properties		VA1	VA2	VA3
Beam		Beam 1	Beam 2	Beam 3
Concentrated Mass	(lb.s ²)/in.	6.55×10^{-3}	6.55×10^{-3}	6.55×10^{-3}
Cross-Sectional Width	in.	1	1	1
Cross-Sectional Height	in.	1/8	1/8	1/8
Area Moment of Inertia	in. ⁴	1.63×10^{-4}	1.63×10^{-4}	1.63×10^{-4}
Beam Length	in.	5.83	6.32	5.39

The three beams are identical in shape but are of different lengths. That is, the three beams have the same cross sections and end masses, but they have different lengths. Because of this, the process of finding, cutting, and preparing the parts is simple. Since the frequencies of the three absorbers are spaced closely, the three beams are very close in length. As shown in Table 3, the difference between the shortest beam ($L_3=5.39$ in.) and the longest beam ($L_2=6.32$ in.) is 0.93 in. This difference in length is relatively miniscule.

It is important to name two lengths for the cantilevered beam that has a slot near the tip: the full length and the effective length. Both are defined in Figure 5.5. The effective length is the distance from the root of the beam to the exact location of the end

mass fastener. The end mass fastener holds the concentrated mass, is near the tip of the beam, and is located within the slot. By creating a slot near the tip of the beam, the end mass fastener can slide easily within the slot. Then, the whole mass can move with it and change its location along the end of the beam.

The effective length also varies due to the change of the position of the mass. After the beam is cut, its full length remains unchanged, but its effective length can change easily. The change in the effective length is restricted by the length of the slot. The variation of the effective length causes the mass to oscillate at different frequencies. These different frequencies are within a particular frequency range. This range depends upon the length of the beam, the location of the slot, and the length of the slot.

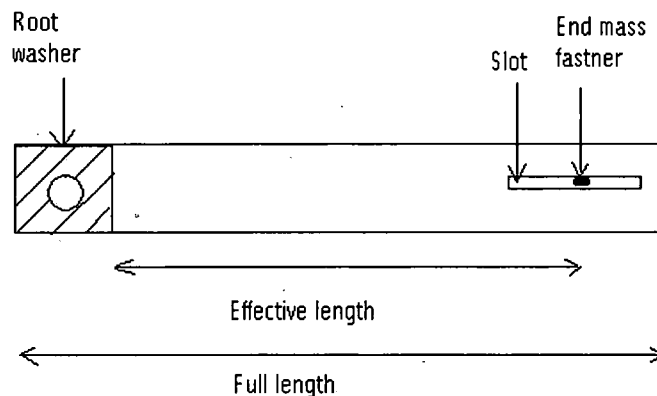


Figure 5.5: Full and Effective Lengths for the Cantilevered Beam

With the appropriate full length (greater than $L_2=6.32$ in.) and the proper slot length (greater than 0.93 in.), three identical beams can be used for the three absorbers. A beam with a full length of 8.08 in. and a slot length of 1.5 in. near the tip has the ability to change its effective length from 5.08 in. to 6.58 in. An absorber with such a beam can be tuned to any frequency within the frequency range of 7.28 Hz to 10.73 Hz. Because the frequencies of the three absorbers are within this frequency range (i.e., $7.28 \text{ Hz} < f_2 < f_1 <$

$f_3 < 10.73$ Hz.), identical beams with the same slot length and location can be used for the three absorbers. Here, 1 in. is used for connecting the root to the square tube. Also, 0.5 in. is left from the end of the slot to the end of the beam.

After theoretically considering the initial design of the 3-DOF TMD, it is important to focus experimentally on the final design. For the final design of the 3-DOF TMD, it is necessary to consider the sandwich beam so that the damping can be introduced to the system. The sandwich beam is constructed from two identical aluminum layers, with an extra-thin layer of viscoelastic damping material between them. Here, only two small pieces of viscoelastic damping material are used. More details will be given later about the damping and the components of the beam.

The next essential step is to determine the full length experimentally. In order to be economical with the beam material and to cut the beam to the appropriate length, the first absorber's end mass fastener is put at the center of the slot. Subsequently, the beam root is clamped to the square tube at a particular position, depending initially on the basis of the theoretical design ($L_1 = 5.83$ in.). Additional attempts may be necessary, and different locations near the beam root are tried until the appropriate full length is determined, as indicated by two new peaks with equal heights in the FRF. Keeping in mind that the frequency is inversely proportional to the square root of the cubic beam length, a slight increase in length may cause a reasonable decrease in the frequency.

After several tries, the full length is determined to be 6.75 in. This full length is suitable for all three beams, including the first. Therefore, the three beams are cut according to the determined full length. Afterward, the effective length needs to be found for each absorber beam through the tuning process.

5.2.1 Absorber Components

Each absorber consists of a cantilevered beam and a mass near its tip. Every uniform beam is composed of two identical aluminum strips, a large bolt with two thick washers at the root, a long bolt with two washers near the tip, and two small pieces of viscoelastic damping material in between. Each strip has a rectangular cross section with a width of 1 in. and a height of 1/16 in. The absorber components (i.e., beam, mass, etc.) with the specified cross-sectional dimensions are shown in Figure 5.6.



Figure 5.6: The Absorber's Components

The aluminum beams without damping treatment (i.e., viscoelastic, coulomb damping) have very low damping (about 2.17%), so viscoelastic material is added to them in order to increase the damping. To provide reasonable damping to the beam system (about 6.8%), only two small pieces of viscoelastic damping material are inserted between the two identical aluminum strips for each beam. Each of the two rectangular viscoelastic pieces has the same width as that of the strips and a length of 1/2 in. Those pieces are placed at 2 in. and 3.5 in. from the root of the cantilevered beam (strip). These pieces act as an individual layer between the two strips, so this beam arrangement slightly increases the moment of inertia and the stiffness of the beam. Because the two pieces are

small (i.e., the sum of their areas covers less than one-fourth of the seam) and extra thin, the role of the two pieces in changing the stiffness is neglected.

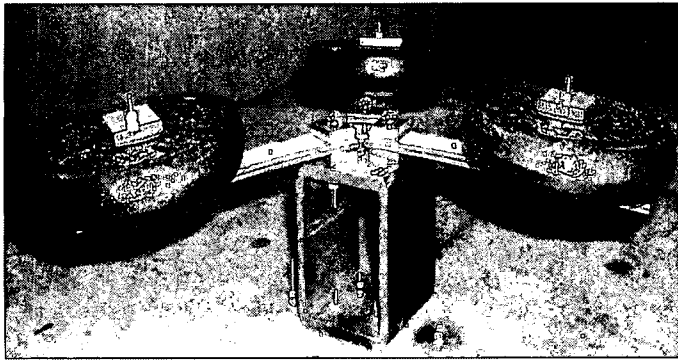
Two thick washers are used at the upper and lower sides of the beam root in order to keep the bending deformation uniform along the beam width. This is done in order for the “cantilevered” assumption of the beam to be valid and so that the boundary conditions for both sides are similar. Also, two washers are put at the lower and upper sides of the beam where the end mass and its fastener (bolt) are located. These washers allow the beam to deflect freely without touching the rigid end mass and also ensure that the deflection in the lower side is similar to the upper side.

Three similar sport weights, which are shaped like rings, are used as end concentrated masses. The masses are 0.75 in. thick, providing sufficient rigidity. Each mass weighs nearly 2.5 lbs. The center of the gravity of this uniform object is at its geometric center (i.e., the middle). The resultant vertical force of the weight is perpendicular to the beam’s axis, near the tip of the beam, and located within the slot.

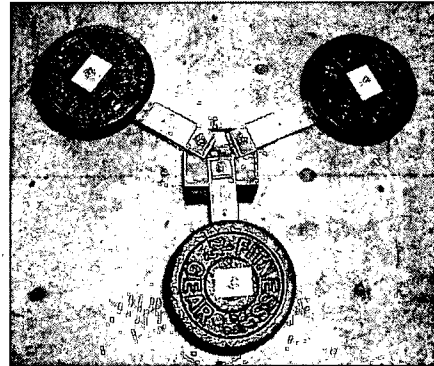
The only types of fasteners used in building the 3-DOF TMD are bolts, but these bolts have different diameters and lengths. The root of the cantilevered beam is bolted to the square tube, and the concentrated mass is bolted at its tip. The diameter of the large bolt at the root of the beam should be at least one-fourth of the beam’s width for the “cantilevered” assumption to be valid. The tip bolt is long enough to go through the concentrated mass, the washers, and the two strips.

The 3-DOF TMD consists of three absorbers in the form of three identical beams with equal concentrated masses near their tips. Figure 5.7 shows the three absorbers of the 3-DOF TMD. The three beams are identical in nearly every way, including slot sizes

and locations near the tips, shape, and material. However, one exception is that the exact position of the end mass fastener within the slot is different from one beam to another. More information will be provided later in the description of the tuning process.



(A) Side View of the 3-DOF TMD



(B) Top View of the 3-DOF TMD

Figure 5.7: The 3-DOF TMD on the Floor Model

To provide the 3-DOF TMD with a good connection to the floor model, a rigid intermediate member needs to be introduced between them. For ease of attachment, the intermediate member is selected to be a square tube in a horizontal position. Because the experimental tests needed for designing and examining the 3-DOF TMD require a series of steps, the square tube and the 3-DOF TMD are placed on the center of the top surface of the floor model. The square tube is held in place to the floor properly by four small bolts near the corners of its lower wall. The wall thickness is 0.19 in., and the outside dimensions of the steel square tube are 2.5 in. by 2.875 in. The square tube behaves as a support for the 3-DOF TMD; therefore, it has thick walls which are made of steel. The walls of the square tube are thicker than the beams of the three absorbers.

5.3 Tuning of the 3-DOF TMD

To tune, experimentally, the absorber to the target mode, the stiffness of the beam system needs to be modified until the desired value is reached. An adjustment to the effective length of the beam, through changing the exact position of the mass near the tip of the beam, is necessary to meet the required stiffness. One way to allow the mass near the tip to change its exact position is by creating a slot near the tip. This slot allows the end mass fastener to slide easily and then the whole mass to change its position along the end of the beam. This provides a convenient way to tune the absorber to the target mode.

Each absorber is tuned individually so that all three are adjusted properly. One way to tune each absorber is to install and tune the absorbers one at a time. Another way is to tune one and restrain the vertical motion of one or both other two absorbers' end masses. This is done with wooden blocks that have a height similar to the square tube height. Wood is suitable for the restraining block because of its light weight.

Because the slot exists near the tip with the right length (slot length = 1.5 in.) and the full length is determined, the tuning process for the three absorbers is simple. The first absorber (VA1) is tuned to the fundamental frequency at 9.375 Hz. The new system after the installation of the first absorber may again have two new peaks with unequal heights. The first absorber is tuned optimally to the target frequency by sliding the end mass fastener slightly within the beam slot until the two new peaks have equal heights in the FRF. With the optimal values, the effective length of the first absorber is 4.5 in. Figure 5.8 shows the frequency response magnitude of the floor scale model with and without the first absorber. The absorber splits the peak of the first mode into two new, smaller peaks at 8.75 Hz. and 10 Hz.

The other two absorbers (VA2 and VA3) are used to target the two new peaks at 8.75 Hz and 10 Hz. The three beams have identical full lengths, slot lengths, and end masses. Additionally, the first absorber's target frequency ($f_1=9.375$ Hz) is the average of the other two absorbers' target frequencies (i.e., $f_{11}=8.75$ Hz and $f_{12}=10$ Hz). Because the fastener of the first absorber's end mass is located in the middle of the slot, the fasteners of the other two absorbers' end masses are near the ends of the slot. The effective lengths for the second and third absorbers are 4.75 in. and 4 in, respectively. Although the three beams have the same full length, they have different effective lengths.

The FRF of Figure 5.8 shows that the 3-DOF TMD provides more damping into the first mode of vibration. Because the four new closely-spaced resonant peaks have nearly equal heights, the 3-DOF TMD is tuned optimally. Figure 5.9 depicts the FRF of Figure 5.8 zoomed over the frequency range of 7.5 Hz to 12.5 Hz. As shown in Figure 5.9, the four new resonant peaks in magnitude are lower than the two recent peaks by about 3 dB and lower than the original peak by about 6 dB. Because the four new peaks have much lower magnitude than the original peak, the 3-DOF TMD is effective in reducing the floor vibration. The equivalent viscous damping ratio of the first mode increased from 5.8% to about 12 %.

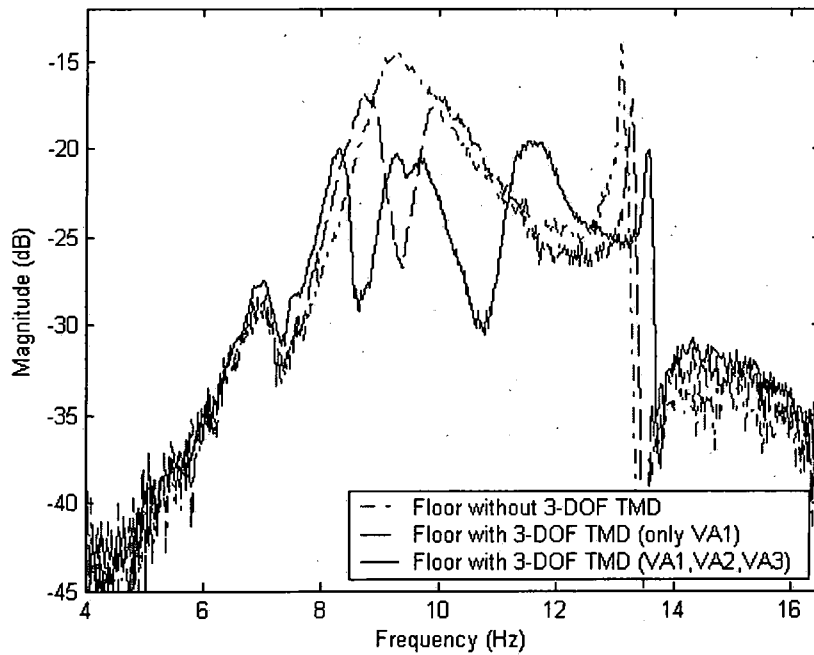


Figure 5.8: Frequency Response Magnitude of the Floor Model With and Without the 3-DOF TMD

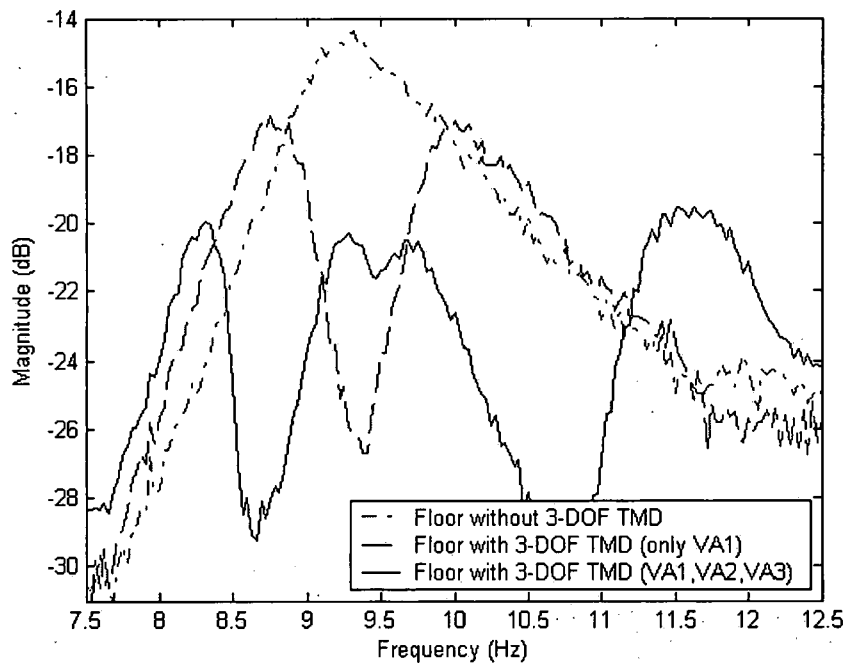


Figure 5.9: Frequency Response Magnitude of the Floor Model With and Without the 3-DOF TMD

CHAPTER VI

SUMMARY, CONCLUSIONS, AND RECOMMENDATIONS

6.1 SUMMARY

Analysis and control of vibration of modern floors are the main thrust of this work. The Virginia Polytechnic Institute laboratory floor, known as VPI floor, which is representative of modern steel-frame, large-span office floors, is used in the numerical analysis portion of this work. A 1/6-scaled version of this floor is fabricated and used for experimental verification of our numerical work. The steel-frame VPI floor is flexible because its concrete slab is thin and made of lightweight material. Also, this floor has very low damping because it has a large, open area without partitions. As a result, the vibration of the VPI floor under normal dynamic loads is very excessive. This structure vibrates at the first natural frequency, 7.3 Hz. Therefore, the floor oscillation is very annoying to the occupants because the natural frequencies of internal human organs fall between 5 Hz. and 8 Hz. Both the Murray criterion [4] and the modified Reiher-Meister scale [10] indicate that the existing VPI floor has an objectionable motion to the occupants.

Among the possible passive and active vibration-control solutions, attaching a passive mechanical device (such as a tuned mass damper, TMD) for reducing the floor vibration seems to be one of the best options and the easiest to implement. A new TMD that has three degrees of freedom and a unique configuration is introduced in this research. The effectiveness of the proposed control scheme is demonstrated numerically on the finite-element model of the VPI floor and experimentally on the 1/6 scaled floor. The proposed 3-DOF TMD has three major subsystems; namely, three absorbers. Each absorber possesses two main structural parts: a cantilevered beam and a concentrated mass at its tip. Every absorber needs a small amount of damping. Two different damping-treatment approaches are presented in this study: coulomb damping and the use of viscoelastic damping material. Overall, the viscoelastic damping approach proves, experimentally, to be more effective than the coulomb damping. The 3-DOF TMD is connected to the scaled floor by an intermediate member, which is selected in this study to be a square tube that lies in a horizontal position.

To reduce the vibration of the VPI floor analytically, a single 3-DOF TMD with 5% mass ratio is designed to control the first vibration mode of the floor at 7.3 Hz. Both the frequency response and the time response show that the 3-DOF TMD introduces a considerable amount of damping into the floor and reduces its vibration. With the 3-DOF TMD, the numerical simulation shows that the first-mode damping ratio of the floor increases from 0.5% to about 7.5%. Similar to the analytical results, the 3-DOF TMD proved, experimentally, to increase the damping of the target vibration mode of the floor scale model.

6.2 CONCLUSION

The 3-DOF TMD with its new configuration has many advantages over the other vibration-control options. The typical TMD usually is placed in the vertical position, upright in the floor, but the proposed TMD is placed in the horizontal position. The three absorbers, in the form of three cantilevered beams with tip masses, expand on a horizontal plane that is parallel to the floor. For the floor applications, it can fit easily into either a ceiling cavity or a small storage space. One of the benefits of using this 3-DOF TMD is that it depends completely upon both basic structural elements (beams, rigid masses, etc.) and several small pieces of viscoelastic damping material. The required structural materials are common and available in the market for a reasonable price; therefore, the cost of the 3-DOF TMD is low by comparison to other passive and active methods. Because the proposed TMD does not need any mechanical device, such as a dashpot, it requires low initial and maintenance expenses. Similar to the typical SDOF TMD, the 3-DOF TMD provides a significant improvement to the floor dynamic response.

On the other hand, the 3-DOF TMD has its disadvantages. In general, it is more sophisticated than the typical SDOF TMD. The 3-DOF TMD has three absorbers; each one has its own structural parts and needs to be tuned to a distinct vibration mode. The process of tuning the three absorbers to the three target modes requires accurate measurements, good experience, and more time. Because the 3-DOF TMD splits the target mode into four closely spaced modes that occupy a wide frequency range (2 Hz. to 4 Hz.), the target mode of the structure must be well-spaced from the neighboring modes.

6.3 RECOMMENDATIONS

To improve and evaluate the effectiveness of the proposed 3-DOF TMD, the following topics are recommended for future research:

1. In order to evaluate experimentally the full effectiveness of the proposed 3-DOF TMD, it is important to consider a structure that has a damping ratio of less than 3%.

2. The three absorbers may need to be rearranged in a new order, their parameters should be optimized, and their damping can have different forms.

3. Because the maximum standard dimension for the thickness of the square tube is about $\frac{1}{2}$ in., it is necessary to search for another structural element with a different cross-sectional shape instead of the square tube. The walls of the square tube should be thicker than the beams of the three absorbers.

REFERENCES

- [1] Velivasakis, E. E., 1997, "LaGuadia High School Gymnasium, Tuned Mass Dampers 'Dance to the Tune' to Tame Floor Vibrations," Proceedings of the First Congress, Minneapolis, MN, ASCE., pp. 198-207.
- [2] Setareh, M., and Hanson, R. D., 1992, "Tuned Mass Dampers for Balcony Vibration Control," J. of Structural Engineering, AISC, **118**, pp. 723-740.
- [3] Webster, A. C., and Vaicaitis, R., 1992, "Application of Tuned Mass Dampers to Control Vibrations of Composite Floor System," Engineering Journal, AISC, **29**, pp. 116-124.
- [4] Murray, T., 1991, "Building Floor Vibration," Engineering Journal, AISC, **28**, pp. 102-109.
- [5] Hanagan, L., 1994, "Active Control of Floor Vibrations," Ph.D. Dissertation, Virginia Polytechnic Institute and State Univ., Blacksburg, VA.
- [6] Rottmann, C. E., 1996, "The Use of Tuned Mass Dampers To Control Annoying Floor Vibrations," M.S. Thesis, Virginia Polytechnic Institute and State Univ., Blacksburg, VA.
- [7] Setareh, M., 1990, "Use of Tuned Mass Dampers for The Vibration Control OF Floors Subjected to Human Movements," Ph.D. Dissertation, The University of Michigan, Ann Arbor, MI.
- [8] Hanagan, L., Murray, T. and Premaratne, K., 2003, "Controlling Floor Vibration with Active and Passive Devices," The Shock and Vibration Digest, **35** (5), pp. 347-365.
- [9] Khoncarly, M., 1997, "Dynamic Response of Floor Systems to Footfall-Induced Vibrations," Ph.D. Dissertation, Case Western Reserve University, Cleveland, OH.

- [10] Lenzen, K. H., 1966, "Vibration of Steel Joist-Concrete Slab Floors," *Engineering Journal*, AISC, **3**, pp. 133-136.
- [11] Rao, S. S., 1995, *Mechanical Vibrations*, Addison-Wesley Publishing, Inc., Reading, MA
- [12] Hanagan, L., and Murray, T., 1997, "Active Control Approach for Reducing Floor Vibrations," *J. of Structural Engineering*, **123**, pp. 1497-1505.
- [13] Steffen, Jr, V. and Rade, D., 2003, "Absorbers, Vibration," *Encyclopedia of Vibration*, Braun, S., 1st Ed., Academic Press, San Diego.
- [14] Shope, R. L., and Murray, T., 1994, "Using Tuned Mass Dampers to Eliminate Annoying Floor Vibrations," *Proceedings of Structures Congress XIII*, ASCE, **I**, pp. 339-348.
- [15] Galambos, T. V., 1988, *Vibration of Steel Joist-Concrete Slab Floors*, Steel Joist Institute, Technical Digest No. 5
- [16] Tipler, P., 1999, *Physics for Scientists and Engineers*, W.H. Freeman, New York
- [17] Ewins, D., 2003, "Damping Measurement," *Encyclopedia of Vibration*, Braun, S., 1st Ed., Academic Press, San Diego.
- [18] Kashani, R., 1998, "The Innovations Approach to Experimental Modeling of Flexible Structures," *ASME J. of Acoustics and Vibration*, **190**, pp. 689-694.
- [19] Soong, T. and Dargush, G., 1997, *Passive Energy Dissipation Systems in Structural Engineering*, Wiley, New York
- [20] Xu, K., and Igusa, T., 1992, "Dynamic Characteristics of Multiple Substructures with Closely Spaced Frequencies," *Earthquake Engineering and Structural Dynamics*, **21**, pp. 1059-1070.
- [21] Zuo, L., and Nayfeh, S., 2003, "The Multi-Degree-of-Freedom Tuned-Mass Damper for Suppression of Single-Mode Vibration under Random and Harmonic Excitation," *ASME 2003 Design Engineering Technical Conferences and Computers and Information in Engineering Conference*, Chicago, Illinois, USA. , , pp.
- [22] Den Hartog, J., 1934, *Mechanical Vibrations*, McGraw-Hill, New York and London.
- [23] Warburlon, G. and Yorinde E., 1980, "Optimum Absorber parameters for Simple System" *Earthquake Engineering and Structural Dynamics*, **8**, pp. 197-217.

- [24] Distefano, III, J., Stubberud, A., and Williams, I., 1995, *Schaum's Outline of Theory and Problems of Feedback and Control Systems*, McGraw-Hill, New York.
- [25] Kuo, B., 1995, *Automatic control systems*, John Wiley & Sons, New York.
- [26] Inman, D., 2001, *Engineering Vibration*, Prentice Hall, New Jersey.
- [27] Inman, D., 1996, *Engineering Vibration*, Prentice Hall, New Jersey.
- [28] Tse, F., Morse, I., and Hinkle, R., 1978, *Mechanical Vibrations: Theory and Applications*, Allyn and Bacon, Boston, MA.
- [29] Inman, D., 2003, "Damping Models," *Encyclopedia of Vibration*, Braun, S., 1st Ed., Academic Press, San Diego.
- [30] Reiher, H., and Meister, F. J., 1931, "The Effect of Vibration on People," (Translation: Report No. F-TS-616-RE H.Q. Air Material Command, Wright Field, Ohio, 1949)

R702031972